Tsunami Hazard Assessment of Snohomish County, Washington

Project Report – Version 3

Draft of April 13, 2020

Randall J. LeVeque, Frank I. González, and Loyce M. Adams
University of Washington

Study funded by Washington State Emergency Management Division

http://depts.washington.edu/ptha/WA_EMD_Snohomish/

This report summarizes a new modeling study done in 2020
and replaces Version 2 from October, 2018.

Contents

Notes on revised results and report **3**

1 Introduction **4**

2 Earthquake Sources **5**
2.1 Cascadia megathrust event CSZ-L1 . . . 7
2.2 Seattle Fault event SF-L . . . 8
2.3 Alaska event AKmaxWA . . . 9

3 Topography and Bathymetry **10**
3.1 1/3 Arc-second DEMs . . . 10
3.2 Coarser DEMs . . . 11

4 Modeling uncertainties and limitations **11**
4.1 Tide stage and sea level rise . . . 11
4.2 Subsidence . . . 11
4.3 Structures . . . 11
4.4 Bottom friction . . . 11
4.5 Tsunami modification of bathymetry and topography . . . 12

5 Study regions **12**

6 Results **16**
6.1 Sample results . . . 16
6.2 Gauge output . . . 20

Appendices **38**

A Data format **38**
A.1 Gauge time series . . . 38

B CSZ L1 model comparisons **39**

C Seattle Fault scenario issues **41**
C.1 The SF-L event . . . 41
C.2 The SF-S event . . . 45

Acknowledgments **49**

References **49**

Notes on revised results and report

This report summarizes the final modeling results for Snohomish County submitted to the Washington State Department of Natural Resources (DNR) in March, 2020, for use in the production of maximum inundation and current speed mapping products.

This is an update of the original modeling reported in Version 2 from October, 2018 [17], which was itself an update of Version 1 from February 2018 [16].

The new modeling uses more recent topography DEMs and new features of the GeoClaw tsunami modeling software. In particular:

- Improved 1/3 arcsecond DEMs have been provided by NCEI that cover most of the study region.
- Greatly improved 1/9 arcsecond DEMs have been provided by NCEI that cover the port of Everett and nearby land, including the Snohomish River Valley. Much of this land is below MHW but protected by dikes or levies.
- The most recent release of GeoClaw, Version 5.7.0, was used in the new study. The original studies used GeoClaw Versions 5.4.1 and 5.5.0. The new version contains a number of improvements listed below.
- GeoClaw now allows initializing most of the dry land below MHW to be dry (with initial water depth $h = 0$). Previously any regions below MHW were initialized with water depth filling up to the MHW level. A marching front algorithm included in GeoClaw allows the identification of land below MHW that should be dry because it is behind dikes. (This fails if the DEM has gaps in dikes.) This addresses a major concern with earlier versions of this study.
- GeoClaw v5.7.0 also allows selecting fgmax points (where the maximum flow depths and other quantities of interest) using the marching front algorithm, selecting only points that are close to shore and/or have elevation below some cutoff. A preliminary version of this feature was used in the earlier studies, but this has been further developed. The efficiency of the code that updates the maxima at these points was also greatly improved. With these changes, it is possible to cover much larger regions with fgmax points in each computer simulation. The portion of Snohomish County covered in this report has thus been split into only 3 study regions rather than 8 as in Version 1 of this study. Version 2 of this study used a preliminary form of these improvements, but still using the 8 study regions from Version 1 plus one additional overlap study region that is also no longer needed.
- The part of Snohomish County north of 48.25N is not included in this new study. This region is roughly north of Highway 20 that runs through Stanwood, WA on the way to Camano Island. Tsunami waves reach this region by a different route than for the rest of Snohomish County, and modeling of this region has been included in modeling the "Skagit Region" in our recent study of portions Island and Skagit Counties [2], which covered all of Skagit Bay.
- In addition to the two events SF-L and CSZ-L1 used in the original study, this report also includes model results for AKmaxWA, a hypothetical Alaska event of magnitude Mw 9.24.

The original versions of this report are found at [19] and can be consulted for results to compare with those presented in this study.

1 Introduction

This report documents the results of a study supported by the Washington State Emergency Management Division of the tsunami hazard along the coast of Snohomish County. Results include inundation depths and times of arrival that will be useful to coastal communities, as well as tsunami current speeds and momentum flux.

A pre-release version of GeoClaw Version 5.7.0 was used for the modeling. This open source software is distributed as part of Clawpack, and is available from [7]. This version contains several enhancements that were developed in response to difficulties that arose in our earlier study of Snohomish County [17] and later work on Whatcom County [1], Bainbridge Island [29], and portions of Island and Skagit Counties [2]. Some of the recent modifications to the code are described in those reports or their appendices.

Figure 1 shows the Snohomish County region and the extents of the three "fgmax grids" on which the results have been provided. In these regions the quantities of interest have been provided as netCDF files on a set of points with 1/3 arcsecond spacing in longitude and 1/3 arcsecond spacing in latitude (approximately 7 m and 10 m respectively). The data format is discussed further in Section A.

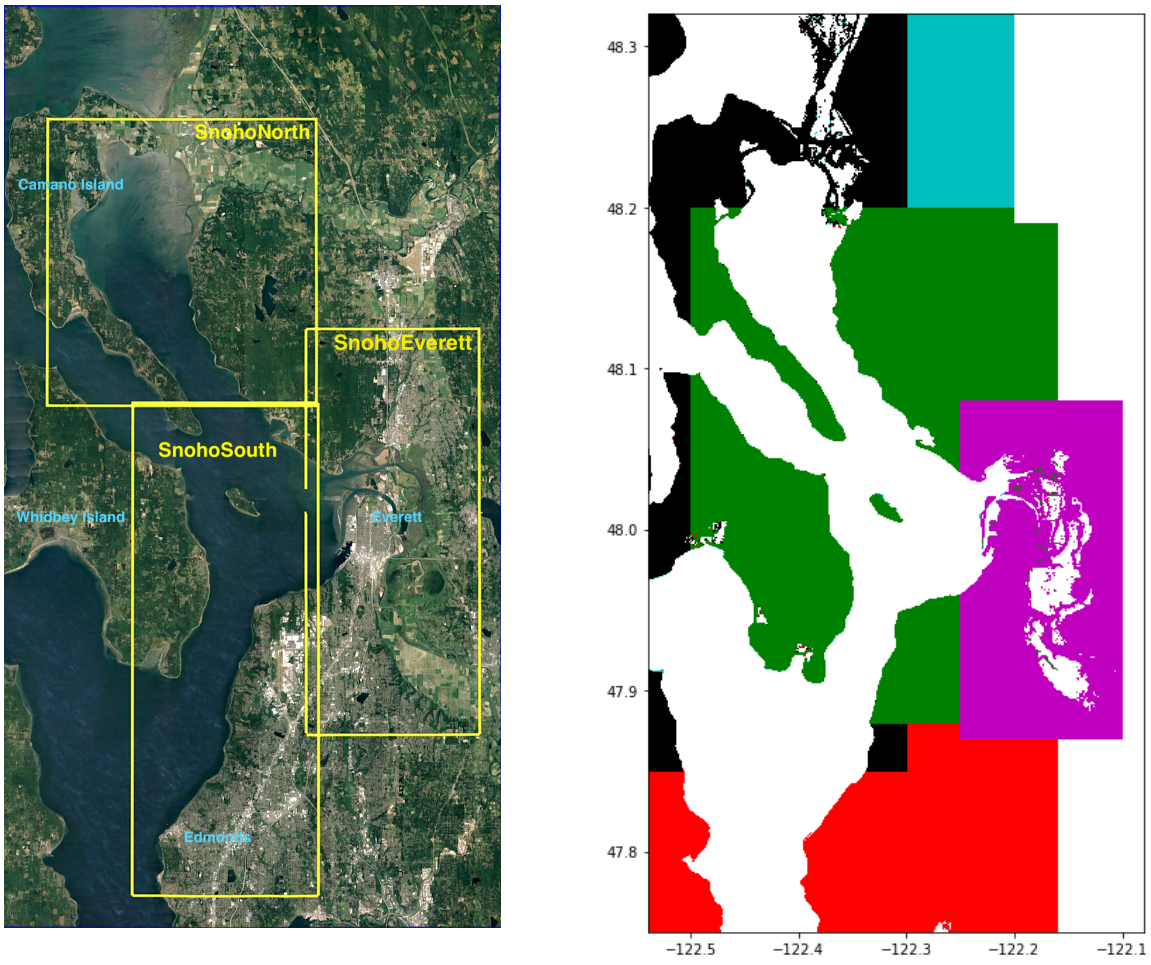

Figure 1: Left: Google Earth image, with the extents of the three study regions shown. Camano Island and Whidbey Island are in Island County, but eastern coasts of these islands are also included in the simulation results. Right: Topography DEM files that were merged for use around Snohomish County (see Section 3). Cyan: Port Townsend, Red: Puget Sound, Black: Merged from 2019, Green: Merged from 2017, Purple: 1/9" around Everett from 2020.

2 Earthquake Sources

Three earthquake sources were considered for this study: a Cascadia Subduction Zone (CSZ) megathurst event with moment magnitude Mw 9.0 (denoted CSZ-L1), a potential Seattle Fault rupture denoted SF-L, and a hypothetical Mw 9.2 event from Alaska (denoted AKmaxWA).

The CSZ-L1 event creates very large waves along the outer coast and a substantial wave that propagates into the Strait of Juan de Fuca (SJdF) and into Puget Sound, affecting parts of Snohomish County with some significant flooding, starting about 2 hours after the earthquake.

The Seattle Fault cuts across Puget Sound (through Seattle and Bainbridge Island) and can create a tsunami that affects the southern portion of Snohomish County almost immediately, and the northern portion within an hour. The larger hypothetical event SF-L considered here would cause significant inundation and high currents in parts of the County.

Waves from the AKmaxWA source reach the Snohomish County region roughly 4 hours after the earthquake. This event generally gives smaller inundation depths and current velocities than the others, but they can still be significant.

Other potential sources have not been considered in this study. Several other fault zones cross Puget Sound as shown in Figure 2 [33]. In particular, the South Whidbey Island Fault (SWIF) cuts through southern Snohomish County, so a tsunami generated by an earthquake on this fault could have significant effect. The SWIF was not included in the statement of work for this project due to lack of a peer-reviewed credible worst case event on this fault, although Mw 7 scenario has been used for seismic hazard studies in the past, e.g. [32].

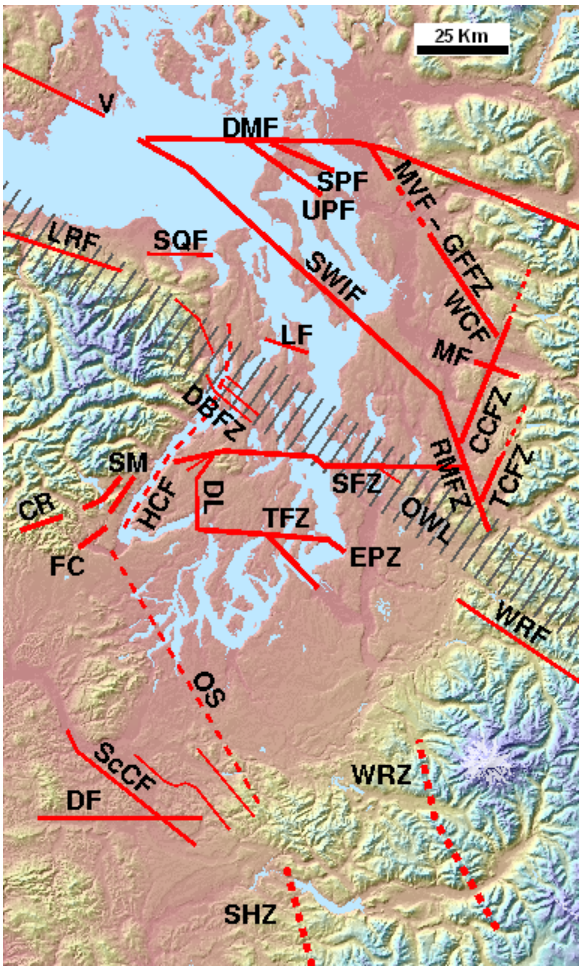

Figure 2: Puget Sound faults, including the Seattle Fault Zone (SFZ). From https://en.wikipedia.org/wiki/File:Puget_Sound_faults.png (CC-BY SA 3.0 License, attributed to J. Johnson and H. Greenberg). See [33] for discussion of the the other faults shown.

2.1 Cascadia megathrust event CSZ-L1

The probability that an earthquake of magnitude 8 or greater will occur on the Cascadia Subduction Zone (CSZ) in the next 50 years has been estimated to be 10-14% (Petersen, et. al., 2002 [24]). The last such event occurred in 1700 (Satake, et al., 2003 [26]; Atwater, et al., 2005 [3]) and future events are expected to generate a destructive tsunami that will inundate Washington Pacific coast communities within tens of minutes after the earthquake main shock. Waves will travel through the Strait of Juan de Fuca and start arriving at Snohomish County coastlines roughly 2 hours after the earthquake.

The potential CSZ event used in this study is the L1 scenerio developed by Witter, et al. (2013) [34]; crustal deformation for the region of interest is shown in Figure 3. The L1 source is one of 15 seismic scenarios used in a hazard assessment study of Bandon, OR, based on an analysis of data spanning 10,000 years. This scenario has been adopted by Washington State as the "worst considered case" for many inundation modeling studies and subsequent evacuation map development; it is used because the standard engineering planning horizon is 2500 years and Witter, et al. (2013) [34] estimated that L1 has a mean recurrence period of approximately 3333 years, with the highest probability of occurrence of all events considered with magnitude greater than Mw 9.

The original L1 source was developed for studies on the Oregon coast and was truncated at around 48N. For past studies on the Washington coast, two different extended versions of this source have been used. One, developed by PMEL, carried the fault farther NW along Vancouver Island. The second, developed by the UW group, instead extrapolated the rupture straight northward from the line of truncation. This is less physical, but potentially directed more wave energy into the Strait. These two deformations are shown in Figure 3.

For this project DNR requested that the PMEL version of the L1 source be used to facilitate comparison with their results. In Version 1 of this study we found that results obtained with the UW version were quite similar. Figure 12 shows a sample comparison of the inundation and currents near Everett when the two versions of L1 are used as sources. A comparison of these sources was also recently performed by Carrie Garrison-Laney of Washington Sea Grant, who also found that similar results were obtained in the regions she considered (Discovery Bay and Hood Canal) [10].

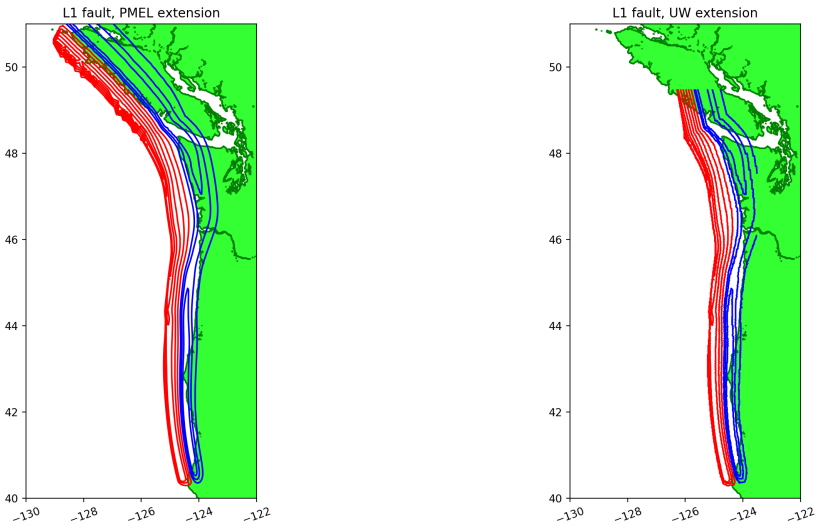

Figure 3: Surface deformation of the L1 source. The PMEL extension used on the left was used in this study, with maximum uplift 15.08 m and maximum subsidence -3.98 m. The UW extension shown on the right has been used in some past studies, with maximum uplift 15.30 m and maximum subsidence -3.99 m. In both figures, red contours show uplift (2 meter interval), blue contours show subsidence (1 meter interval).

2.2 Seattle Fault event SF-L

Figure 4 shows contours of uplift and subsidence due to a hypothetical event on the Seattle fault that we denote by SF-L. Earlier tsunami hazard studies have referred to this as a Mw 7.3 event. However, when we tried to recreate the deformation field by applying the Okada model to the subfault parameters listed in [5], we determined that the magnitude should be Mw 7.54, as discussed further in Appendix C. Regardless of the proper magnitude, we are using the deformation file provided by PMEL that has been used for the previous tsunami hazard analyses of Everett [5].

Due to uncertainty about the magnitude, we adopted the SF-L notation for this larger Seattle Fault scenario. The deformation was originally chosen to match observed uplift and subsidence at a few points around Puget Sound. Since the original specification of this deformation, many new observations have been made and improved models for the subfault geometry have also been produced. A new model for SF-L is now under development and in the future this will be used to update the results of the current study.

A smaller Seattle Fault scenario (SF-S) was also initially considered, but even more uncertainty arose over the proper specification of fault slip for this event, and so this has not been used in the present study. Appendix C contains some discussion of difficulties with this scenario, for future reference. Some preliminary simulations with different versions of SF-S showed very little inundation and few regions of high currents in Snohomish County (see Figure 18 for one sample result). A new SF-S source is also currently under development that may be used in future tsunami hazard assessment.

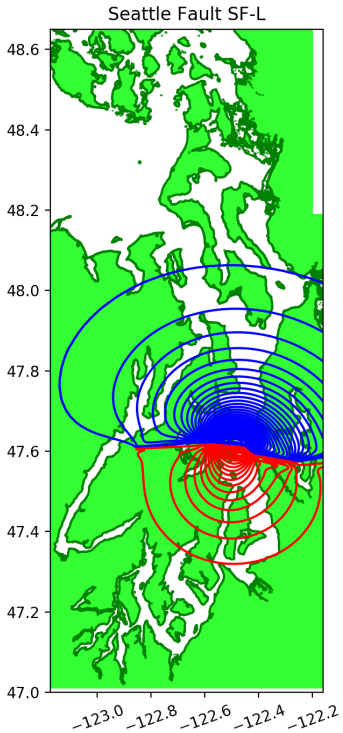

Figure 4: Surface deformation for Seattle Faulte event SF-L. The blue contours show subsidence at levels -0.05, -0.1, ... meters, with maximum subsidence -1.78m. The red contours show uplift at levels 0.5, 1, 1.5, ... meters, with maximum uplift 8.37m.

2.3 Alaska event AKmaxWA

The Aleutian Subduction Zone event denoted by AKmaxWA in this study is based on a hypothetical earthquake developed by PMEL in the work reported in [6], shown in Figure 5. (This source was not included in Versions 1 or 2 of this study.) The AKmaxWA source was designed to have a similar magnitude and location as the 1964 Alaska Earthquake (Mw 9.2) but to have uniform slip of 20 m specified over a set of 20 "unit source" subfaults from the NOAA SIFT database. See [2] for more discussion of the development of this source.

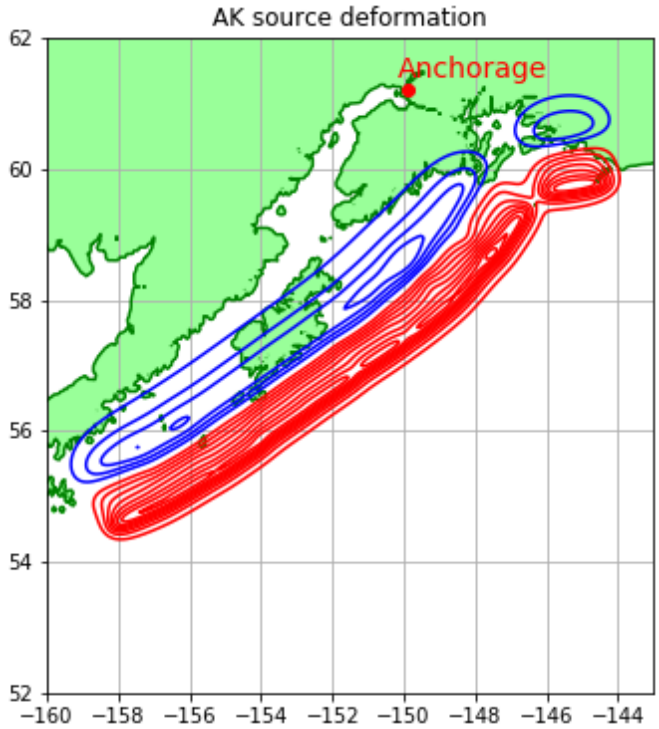

Figure 5: Surface deformation of the AKmaxWA source, with maximum uplift 9.7 m and maximum subsidence −4.9 m. Red contours show uplift, blue contours show subsidence (1 meter intervals in each case).

3 Topography and Bathymetry

3.1 1/3 Arc-second DEMs

Output from the model was requested at grid points spaced 1/3" in longitude and 1/3" in latitude, with the points aligned with cell centers of the 1/3" DEM files that are available for the Puget Sound region. (Note that 1/3" in latitude is approximately 10.3 m. At this latitude, 1/3" in longitude is approximately 6.9 m).

GeoClaw uses finite volume methods with adaptive mesh refinement, and the finest grid resolution near regions of interest was set to the desired resolution of 1/3" by 1/3".

Unfortunately there is no single DEM that provides 1/3" topography and bathymetry for all of Snohomish County. The Puget Sound 1/3 Arc-second MHW Coastal Digital Elevation Model [22] (referred to below as PS-DEM) only extends up to 48.19N, while the Port Townsend 1/3 Arc-second MHW Coastal Digital Elevation Model [21] (referred to below as PT-DEM) only extends as far south as 47.91N. Moreover, we found that these two DEMs did not agree well in the region where they overlap, with offshore values differing by nearly 1 m (while onshore values often agreed).

In 2017, for Version 1 of this study [16], NCEI provided a custom merged DEM extending from 47.88N to 48.2N that smoothly matches the PS-DEM to the south and the PT-DEM to the north, and that uses the best available data.

In 2019, for the study of portions of Island and Skagit Counties [2], a new merged DEM was provided by NCEI that covered most of those counties.

In 2020, NCEI provided a new 1/9" DEM that covers Everett and much of the Snohomish River Valley at higher resolution and using improved data sources. This DEM extends east to -122.21, also providing better coverage than earlier DEMs.

For this project the 1/9" DEM was subsampled to 1/3" resolution and then all of these DEMs were merged into a single 1/3" `SnohoMerged` DEM, using the best available data in each region, as indicated in Figure 1.

3.2 Coarser DEMs

The 1/3" PT-DEM and PS-DEM discussed above were also coarsened to obtain 2" DEMs for a larger region. These DEMs are more efficient to use in GeoClaw on coarser grid levels where all the details of the 1/3" DEMs are not required. In addition to these two DEMs, for simulations of the CSZ L1 event, a 2" DEM of the Strait of Juan de Fuca was used that was obtained by coarsening the 1/3" Strait of Juan de Fuca DEM [23]. Outside of the Strait and sound, etopo 1-minute topography for the Pacific Ocean and outer coasts was used.

4 Modeling uncertainties and limitations

The simulations of tsunami generation, propagation and inundation were conducted with the GeoClaw model. This model solves the nonlinear shallow water equations, has undergone extensive verification and validation (e.g. [4, 18], and has been accepted as a validated model by the U.S. National Tsunami Hazard Mitigation Program (NTHMP) after conducting multiple benchmark tests as part of an NTHMP benchmarking workshop [11].

Several important geophysical parameters must be set in the GeoClaw software, and some physical processes are not included in these simulations, which use the two-dimensional shallow water equations. These are discussed below along with their potential effect on the modeling results.

4.1 Tide stage and sea level rise

The simulations were conducted with the background sea level set to MHW. This value is conservative, in the sense that the severity of inundation will generally increase with a higher background sea level. Larger tide levels do occasionally occur, but the assumption of MHW is standard practice in studies of this type. Potential sea level rise over the coming decades was not taken into account in this modeling.

4.2 Subsidence

The Seattle Fault event SF-L causes some subsidence of the study area: the negative deformation contours shown in Figure 4 extend into Snohomish County. This subsidence is accounted for in the GeoClaw modeling, in which the initial topography is modified by the earthquake deformation. This feature is now supported in GeoClaw v5.7.0.

4.3 Structures

Buildings were not included in the simulations, the topographic DEMs provided for this study are "bare earth". The presence of structures will alter tsunami flow patterns and generally impede inland flow. To some extent the lack of structures in the model is therefore a conservative feature, in that their inclusion would generally reduce inland penetration of the tsunami wave. However, as in the case of the friction coefficient, impeding the flow can also result in deeper flow in some areas. It can also lead to higher fluid velocities, particularly in regions where the flow is channelized, such as when flowing up streets that are bounded by buildings.

4.4 Bottom friction

Mannings coefficient of friction was set to 0.025, a standard value used in tsunami modeling that corresponds to gravelly earth. This choice of 0.025 is conservative in some sense, because the presence of trees, structures and vegetation on the coast would justify the use of a larger value, which might tend to reduce the inland flow. On the other hand, larger friction values can lead to deeper flow in some areas, since the water may pile up more as it advances more slowly across the topography. A sensitivity study using other friction values has not been performed.

4.5 Tsunami modification of bathymetry and topography

Severe scouring and deposition are known to occur during a tsunami, undermining structures and altering the flow pattern of the tsunami itself. Again, this movement of material requires an expenditure of tsunami energy that tends to reduce the inland extent of inundation. On the other hand, if natural berms or ridges along the coastline (or man-made levies or dikes) are eroded by the tsunami, then some areas can experience much more extensive flooding. There is no erosion or deposition included in the simulations presented here.

5 Study regions

The coast of Snohomish County was subdivided into three regions, as shown in Figure 1. These will be referred to as *fgmax regions* since these are regions on which a fixed grid is defined (independent of adaptive refinement) on which the maximum of each quantity of interest is monitored during the course of the simulation. The quantities monitored are the flow depth, flow speed, and momentum flux, along with the time at which the maximum is attained and the first arrival time of significant waves at each grid point. In addition, the minimum water depth at each point is monitored, which can be useful to know in ports or marinas where boats may be grounded. For each earthquake event considered, 3 different GeoClaw runs were performed, one focusing on each of these regions.

The fgmax points lie on a grid with spacing 1/3" by 1/3" that is aligned with the DEM grids. The improved version of GeoClaw v5.7.0 allows selecting only the grid points in each region for which the topography elevation is below some limit, here taken to be 15 m, and in addition the point is connected to the open water by a path that lies below this elevation. We assume that points with greater elevation will not be inundated from any of the events considered — a good assumption since inundation depths were a few meters at most. In Versions 1 and 2 of this project the elevation 40 m was used to select fgmax points in order to insure a buffer of dry points exists around the inundation region, particularly along the shore in regions of steep topography. The improved version of GeoClaw v5.7.0 also allows specifying a buffer zone separately and the we enforce that the fgmax grids include at least 10 grid points in from the shoreline.

If only onshore inundation and near shore currents need to be modeled, then one could also set a lower threshold, e.g. -40 m, and only select grid points where the bathymetry elevation is above this value. For this project we included all water points in order to model currents off shore.

Region label	West	East	South	North	Count	Figures
SnohoNorth	-122.375	-122.25	48.073	48.25	2,195,033	6, 9
SnohoEverett	-122.26	-122.10	47.87	48.12	1,791,323	7, 10
SnohoSouth	-122.42	-122.249	47.77	48.075	3,164,479	8, 11
Total					7,150,835	

Table 1: The three fgmax regions, listed from north to south. The fgmax points are aligned with the DEM in the regions specified, with 1/3" spacing in longitude and 1/3" in latitude. Only grid points for which the topography elevation is less than 40 m were used, and the column labeled "Count" gives the number of fgmax points in each region. See Figures 6–8 for plots of the fgmax max points colored by elevation, and Figures 9– 11 for plots of the simulation results.

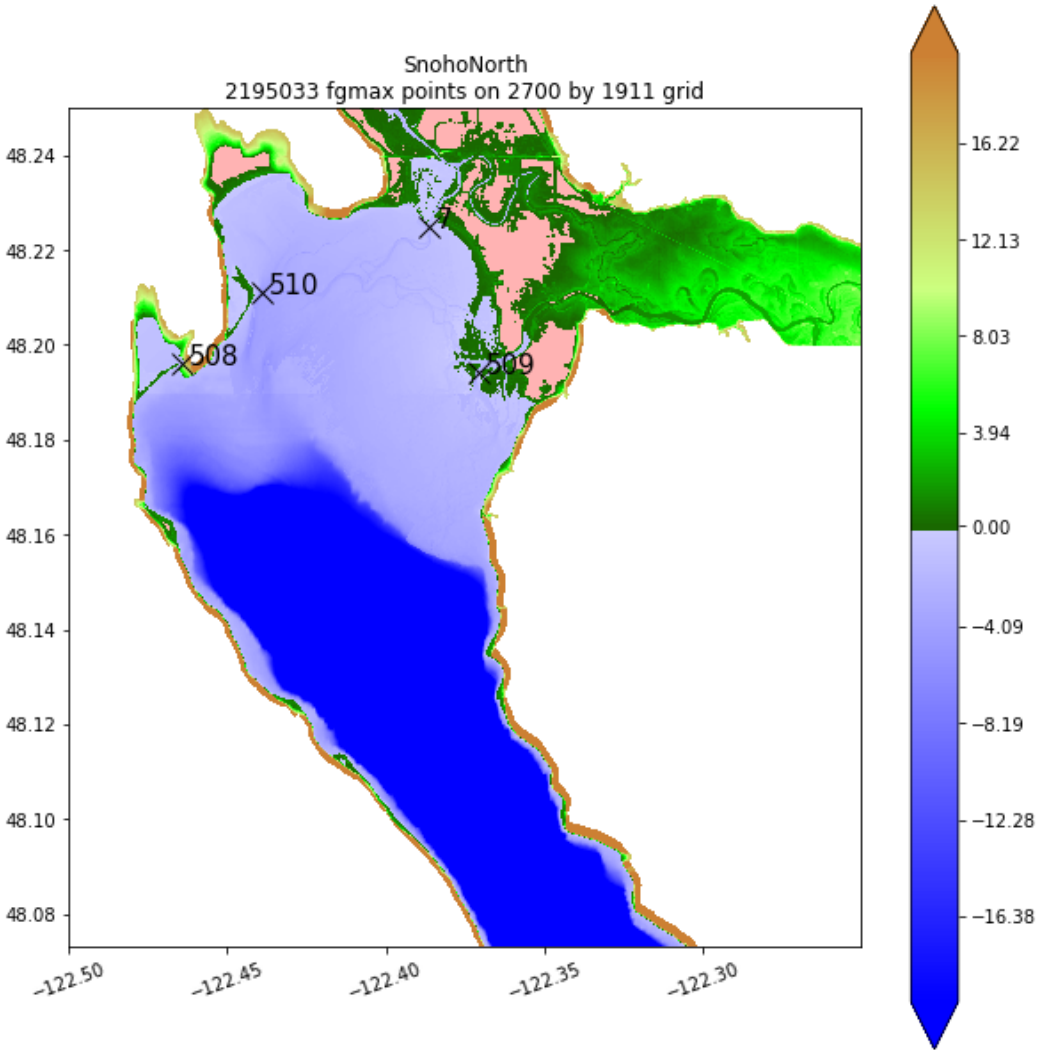

Figure 6: The topography elevation at the fgmax points for region SnohoNorth. Regions in pink are dry land below MHW (protected by dikes or levies). Locations of synthetic gauges in this region are also shown at × points. See Section 6.2.

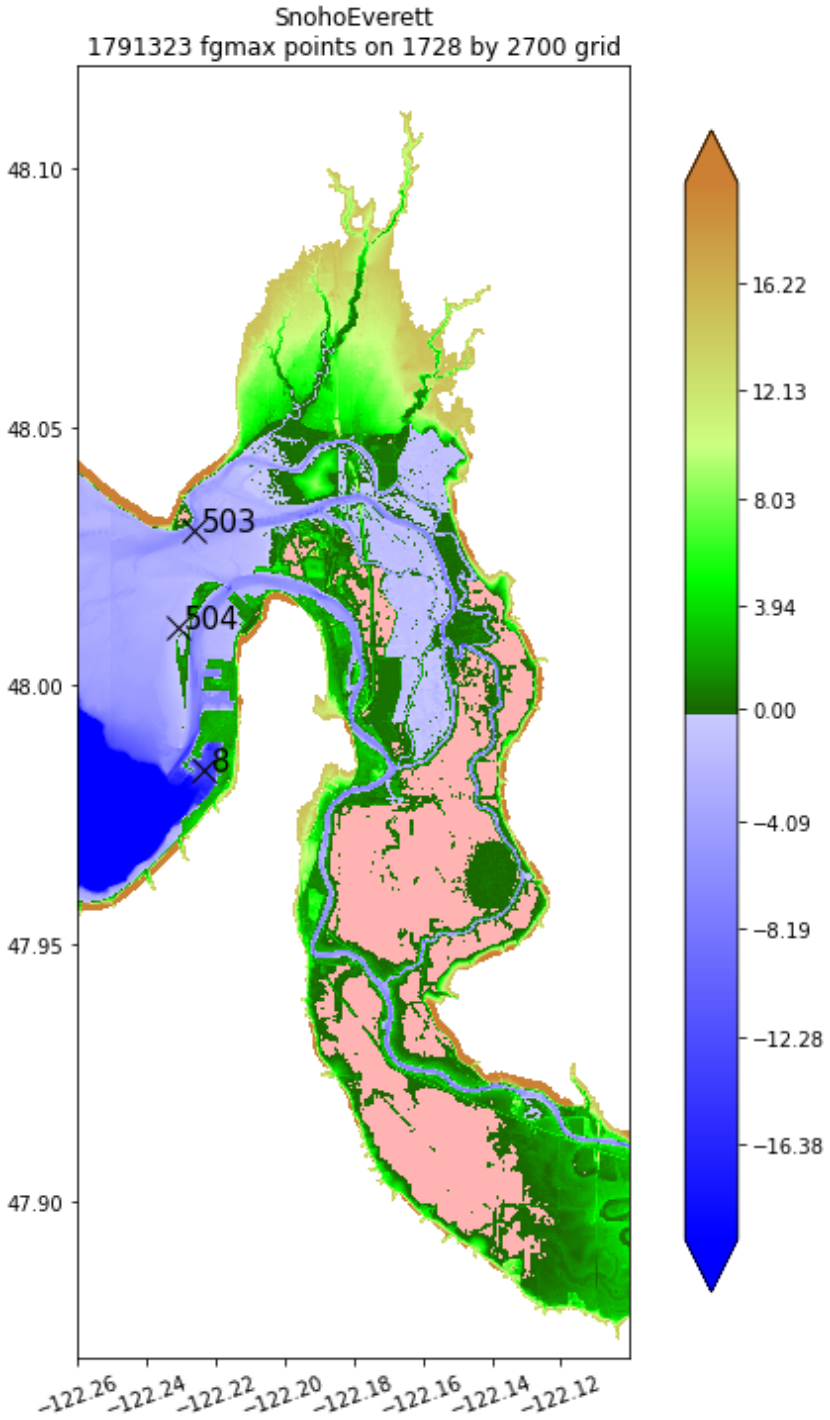

Figure 7: The topography elevation at the fgmax points for region SnohoEverett. Regions in pink are dry land below MHW (protected by dikes or levies). Locations of synthetic gauges in this region are also shown at × points. See Section 6.2.

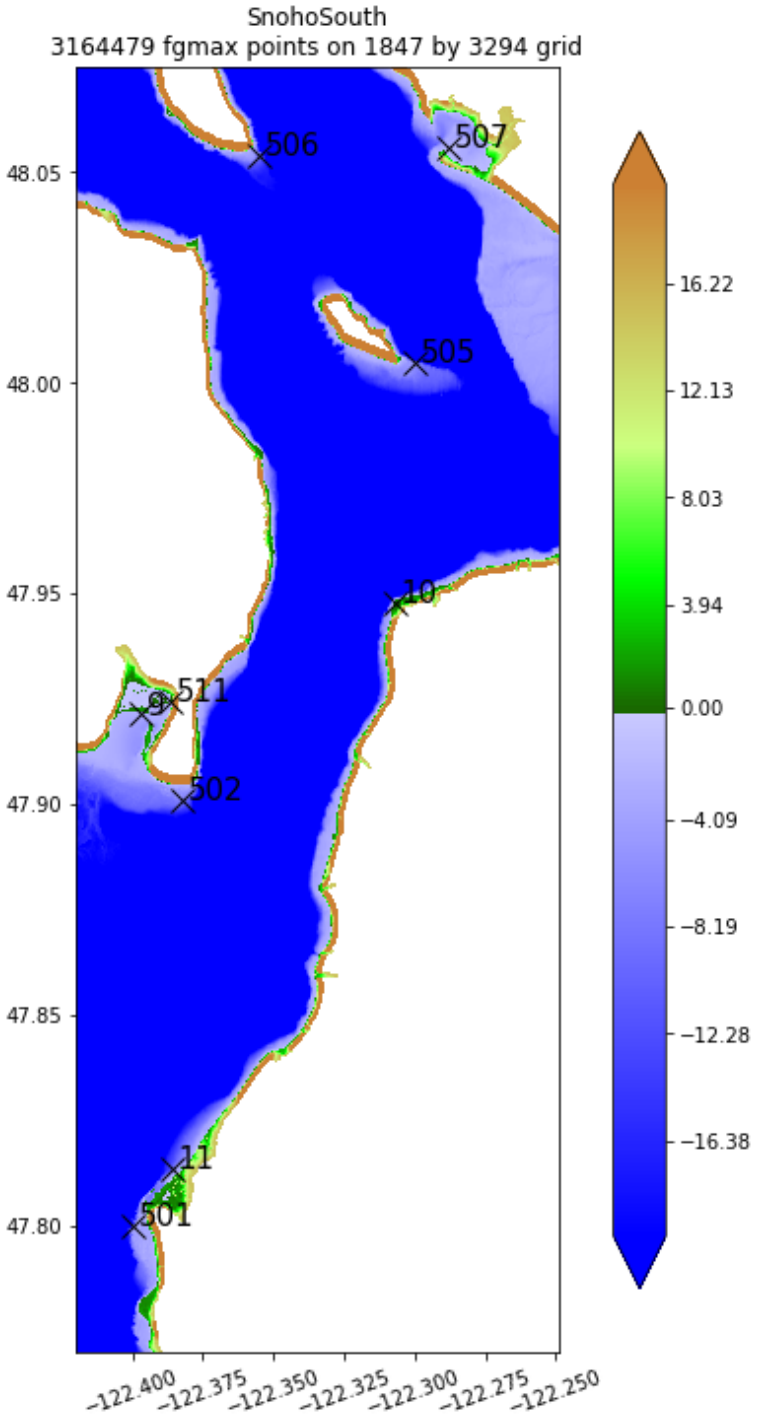

Figure 8: The topography elevation at the fgmax points for region SnohoSouth. In this region there is no dry land below MHW. Locations of synthetic gauges in this region are also shown at × points. See Section 6.2.

6 Results

6.1 Sample results

Some sample results are shown in Figures 9 through 11. We have not attempted to produce high quality graphics of the results, since Washington State DNR is taking our raw data and producing the maps that will be published elsewhere. However, we provide some plots to give an indication of the sort of flooding and flow speeds observed, and for future reference if the simulations are re-run at a later date.

Plots of these fgmax results along with additional plots of other quantities are also available in the form of a `.kmz` file containing kml wrappers to allow visualizing the results on Google Earth or related platforms. This allows zooming in on the region of interest much more easily than trying to view fine scale features of the plots below. These files are available for download from [20].

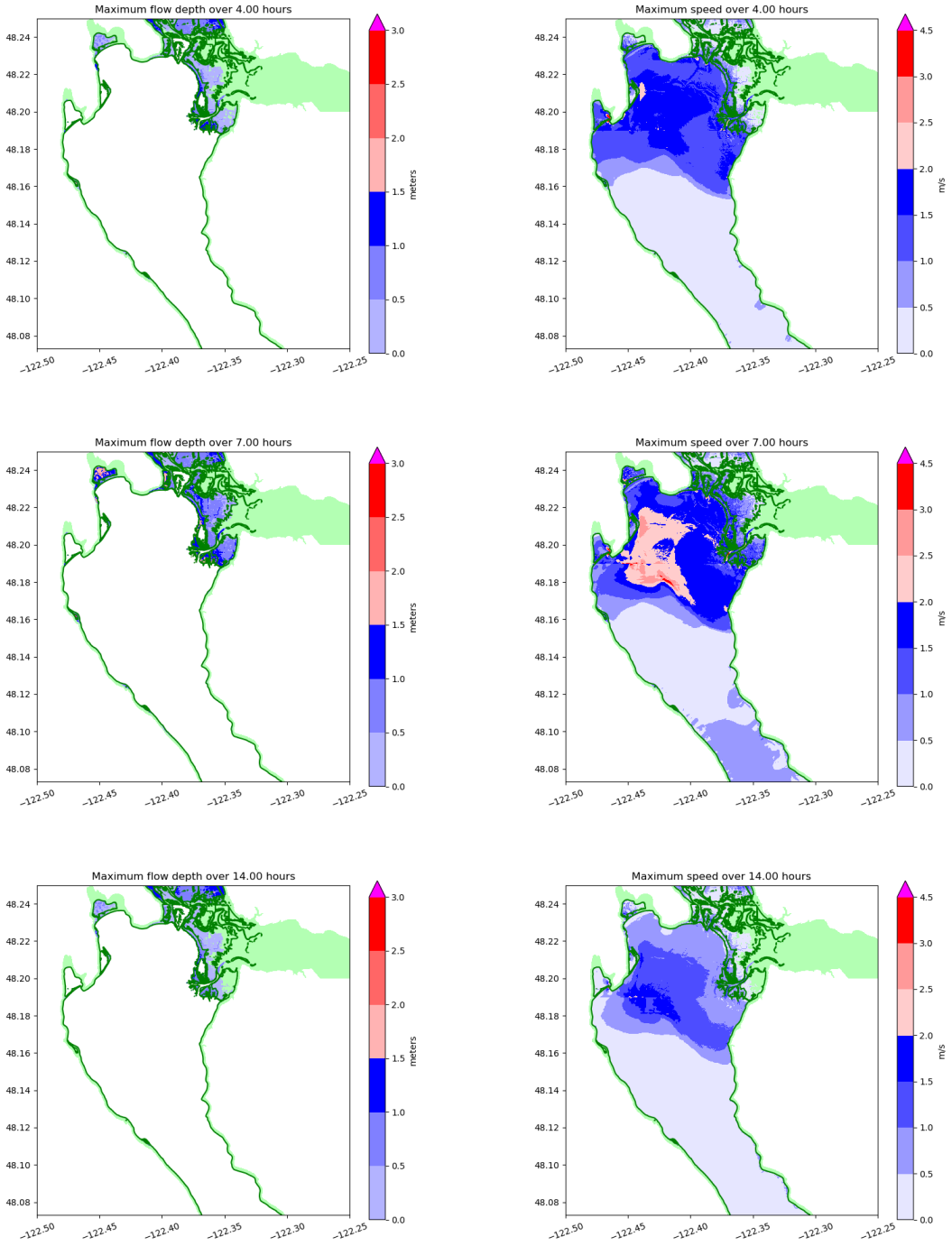

Figure 9: Sample results for the Region `SnohoNorth` for all three events. **Top:** SF-L, **Middle:** CSZ-L1, **Bottom:** AKmaxWA. **Left:** Depth, **Right:** Speed. Green regions are where there were fgmax points that remained dry.

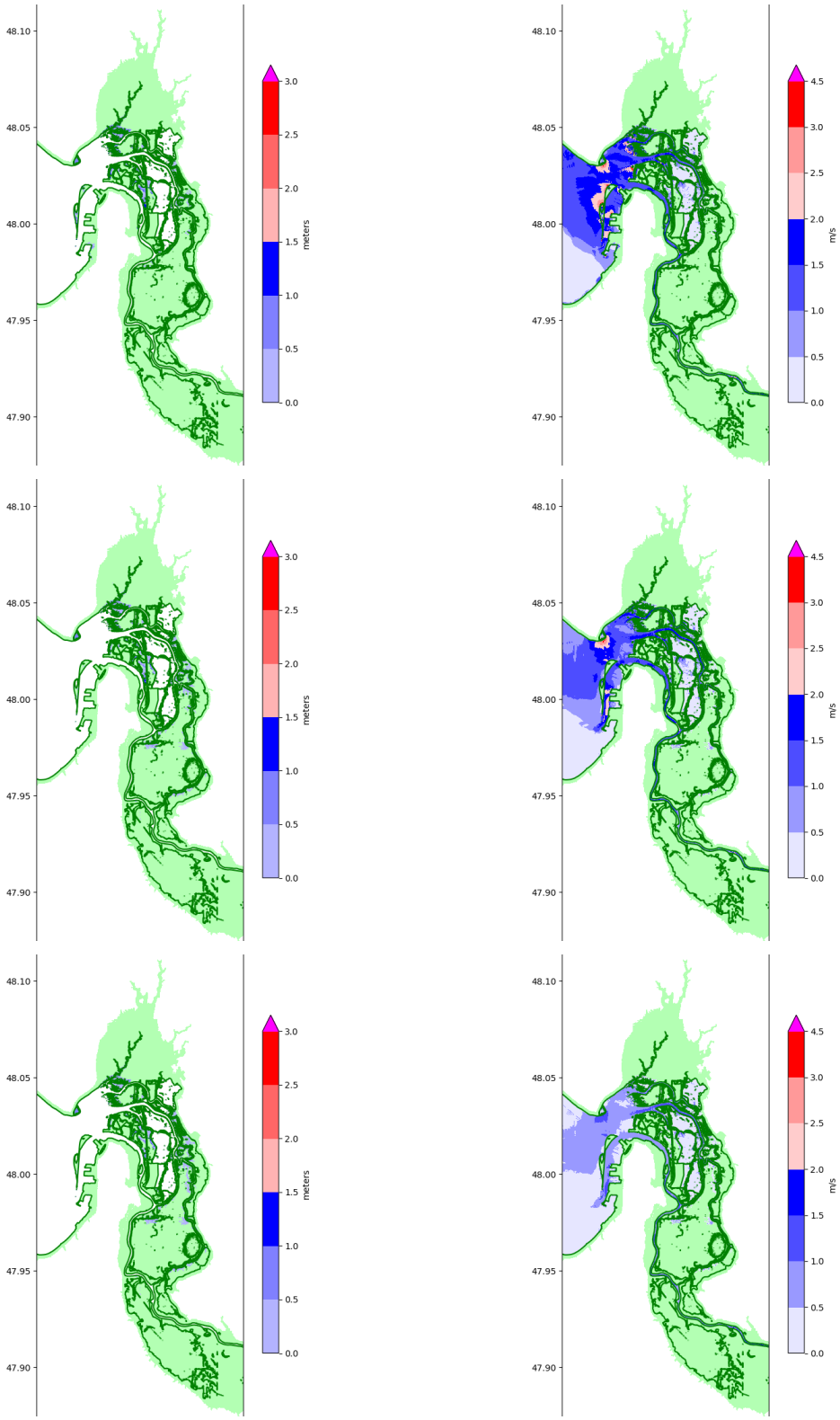

Figure 10: Sample results for the Region `SnohoEverett` for all three events. **Top:** SF-L, **Middle:** CSZ-L1, **Bottom:** AKmaxWA. **Left:** Depth, **Right:** Speed. Green regions are where there were fgmax points that remained dry.

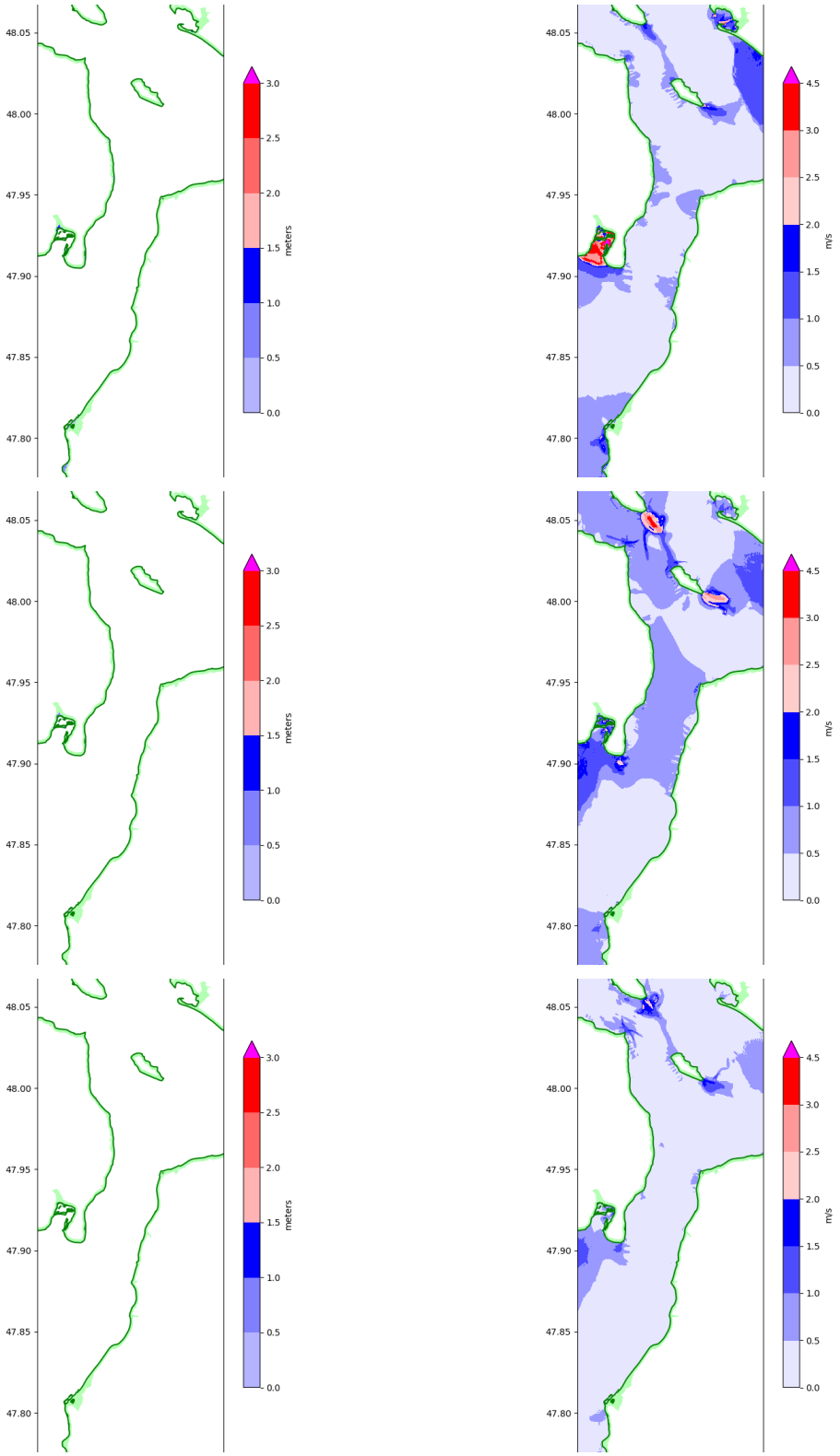

Figure 11: Sample results for the Region `SnohoSouth` for all three events. **Top:** SF-L, **Middle:** CSZ-L1, **Bottom:** AKmaxWA. **Left:** Depth, **Right:** Speed. Green regions are where there were fgmax points that remained dry.

6.2 Gauge output

Table 2 shows the location of simulated gauges used to capture time series of the flow depth / surface elevation and of the current velocity over the course of each simulation. The locations of the gauges are also indicated in Figures 6–8.

Gauges 7–11 were specified by DNR and the remaining gauge locations were chosen at points where the maximum current velocity was particularly large. Examining these gauges gives an indication that the run times chosen for these simulations were sufficiently long to capture the maximum depth and speed at each point.

Note that prior versions of this report also included a Gauge 6 (Skagit Bay South) located in Skagit Bay north of Stanwood, WA. This gauge was not included in the present study since Skagit Bay was instead modeled as part of the recent study of portions Island and Skagit Counties [2], which covered all of Skagit Bay.

Number	Longitude	Latitude	Location
7	-122.3861848	48.2248873	Port Susan
8	-122.2233282	47.9835954	Port Gardner east waterway
9	-122.3969815	47.9213880	Cultus Bay
10	-122.3069525	47.9479784	Mukilteo Lighthouse Park
11	-122.3858967	47.8134986	Edmonds Ferry Terminal
501	-122.4000000	47.8000000	South of Edmonds
502	-122.3820000	47.9010000	SE of Cultus Bay
503	-122.2260000	48.0300000	Priest Point
504	-122.2310000	48.0110000	Jetty Island
505	-122.3000000	48.0050000	SE of Hat Island
506	-122.3550000	48.0540000	SE of Camano Island
507	-122.2880000	48.0560000	Tulalip Bay
508	-122.4643000	48.1960000	Driftwood Shores Camano
509	-122.3705000	48.1940000	Stillaguamish River outlet
510	-122.4390000	48.2110000	Iverson Trail Camano
511	-122.3864000	47.9244000	Inner Cultus Bay

Table 2: Location of synthetic gauges.

The figures on the next few pages show gauge output from the gauges specified in Table 2. The time series for the gauges is available as netCDF files in the data products, as described in Section **??**.

For each gauge, the figures below show results for the SF-L, CSZ-L1, and AKmaxWA events. The left panel in each figure shows the water elevation as a function of time, along with the GeoClaw topography value in the grid cell containing the gauge. This is generally constant in time and shows the initial depth of water at the gauge location.

The right panel in each figure shows the current speed as a function of time along with the time history in the u–v plane, which shows how the direction of flow varies with time.

Note that the gauge plots for the SF-L event generally start at $t = 120$ seconds after the earthquake (which was assumed to have instantaneous displacement) and so the topography elevation shown by the green curves is the elevation after subsidence, if any. For the CSZ L1 event, the gauge time series generally start at 17 minutes post-quake, while for the AKmaxWA event they start roughly 4 hours after the earthquake. There is no subsidence in Snohomish County from the latter two events and so the GeoClaw topography elevation shown for these event is slightly larger than for the SF-L event for the southern gauges where the SF-L source gave subsidence.

Gauge results are generally quite consistent with those reported in previous versions of this study for the SF-L and CSZ-L1 events. Disagreements are thought to be mainly a result of the use of new and improved topography files. Note that the elevation of some gauges has changed, and in particular Gauge 10 (Mukilteo Lighthouse Park) is at an elevation of roughly 1.3 m in the new study and the tsunami does not reach this point from any of the three events. In the previous studies the pre-subsidence elevation was only 0.3 m and

both the SF-L and CSZ-L1 events led to some flooding at this location.

Gauge 7: Port Susan.

Computed on region `SnohoNorth`.

SF-L event:

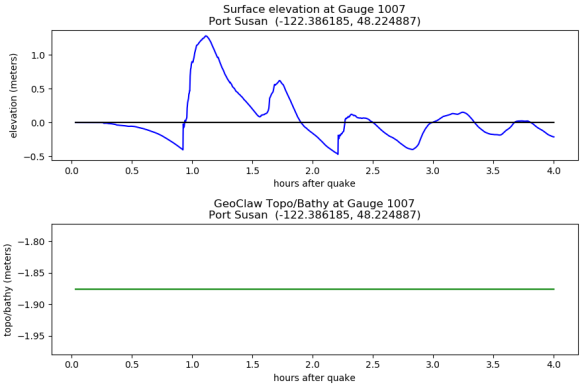

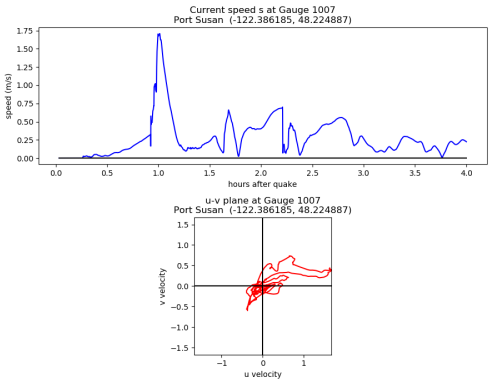

CSZ L1 event:

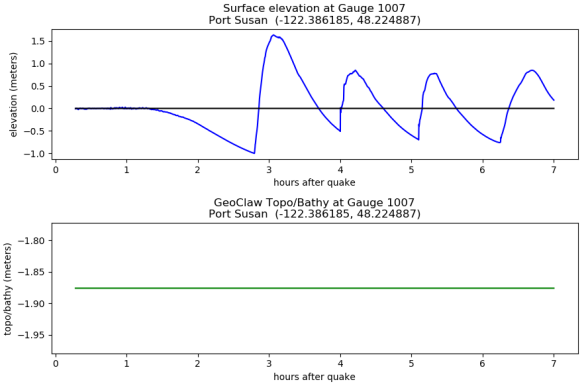

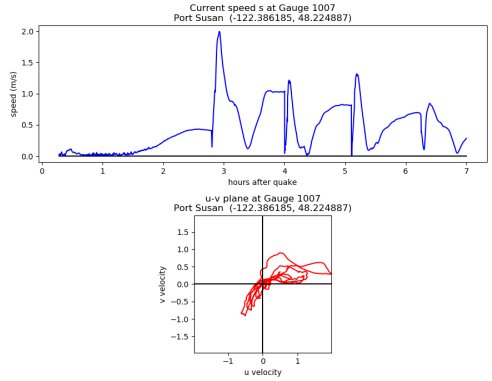

AKmaxWA event:

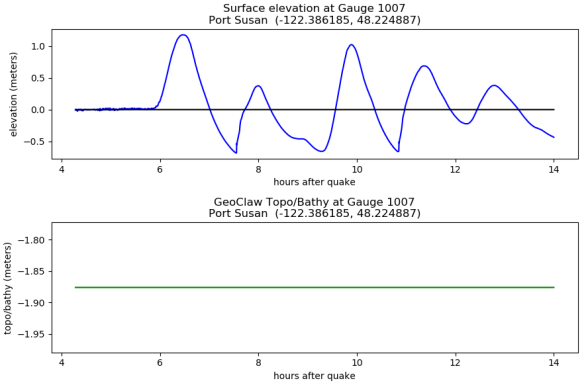

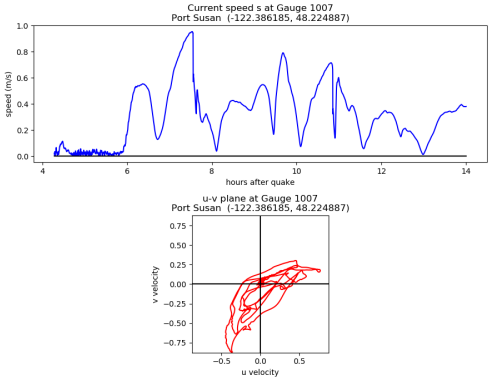

Gauge 8: Port Gardner east waterway.

Computed on region `SnohoEverett`.

SF-L event:

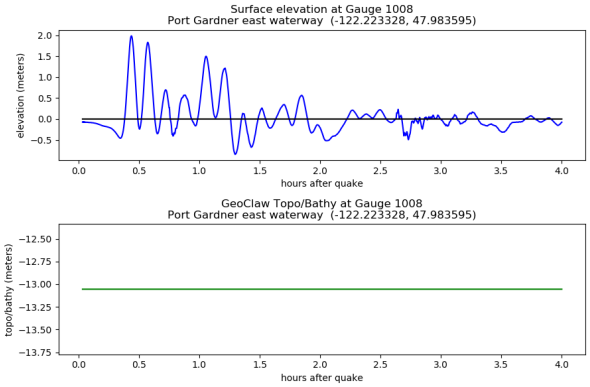

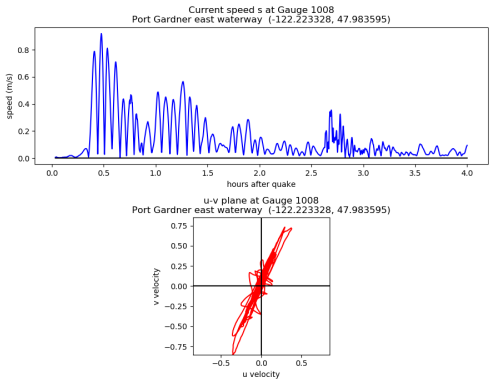

CSZ L1 event:

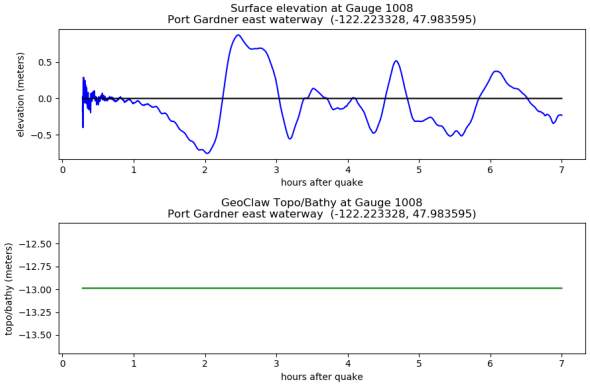

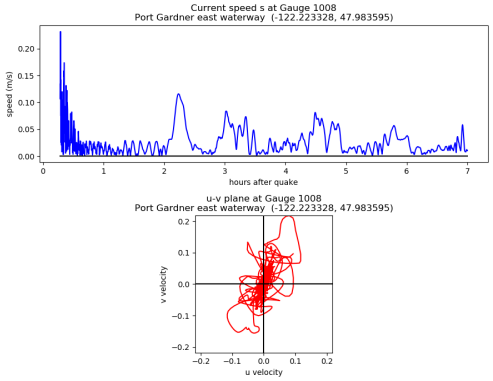

AKmaxWA event:

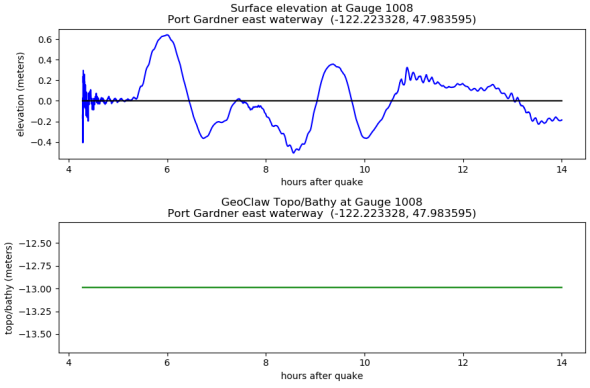

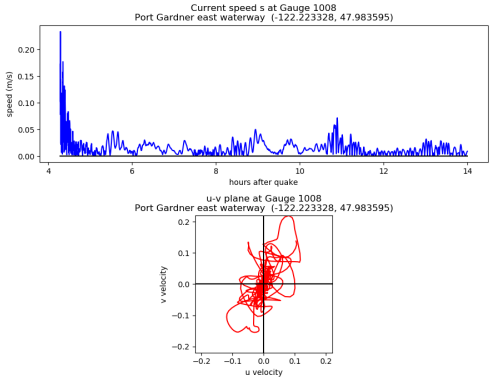

Gauge 9: Cultus Bay.

Computed on region `SnohoSouth`.

SF-L event:

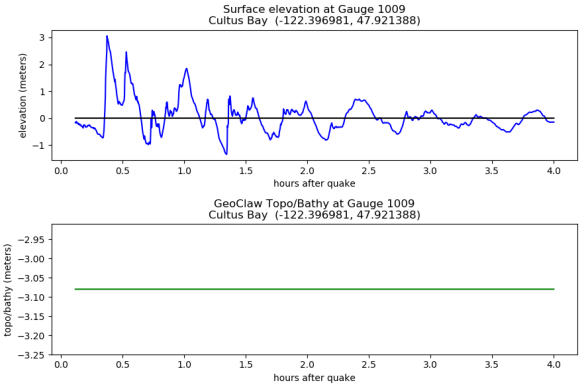

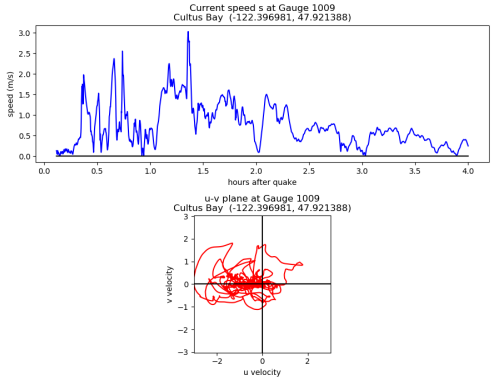

CSZ L1 event:

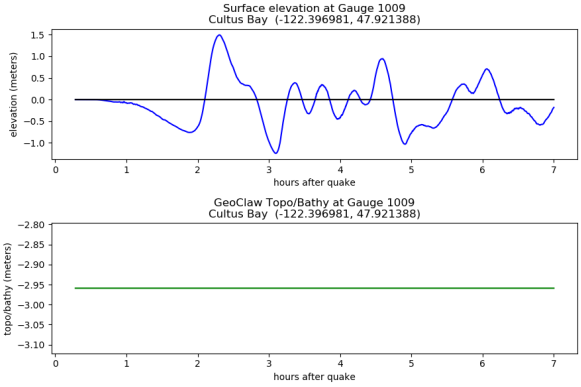

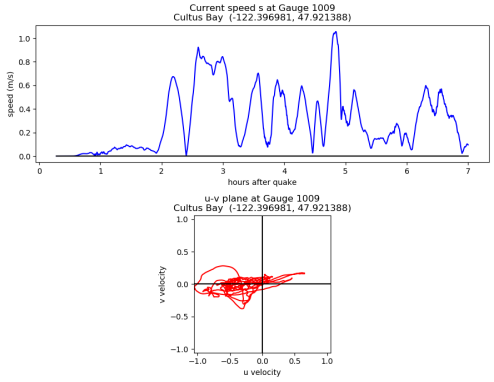

AKmaxWA event:

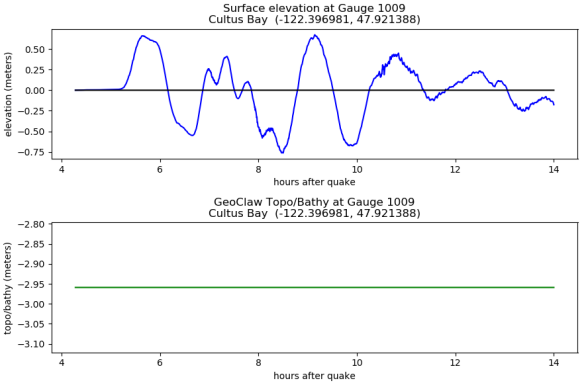

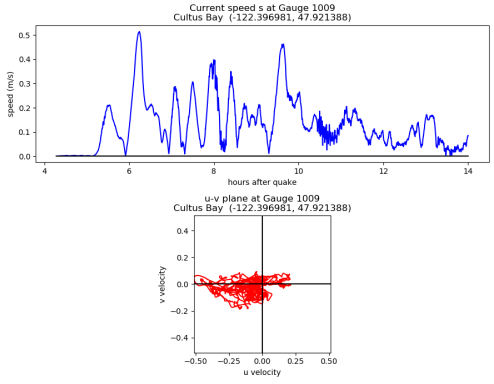

Gauge 10: Mukilteo Lighthouse Park.

Computed on region `SnohoSouth`.

SF-L event:

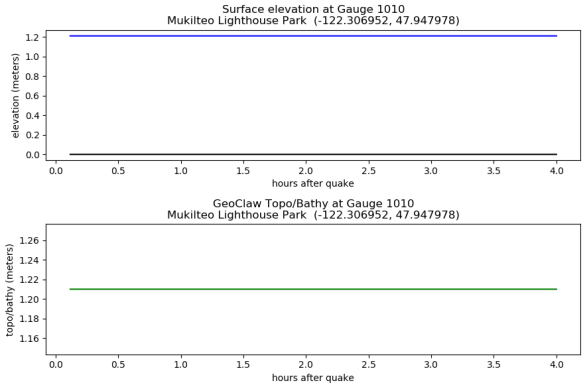

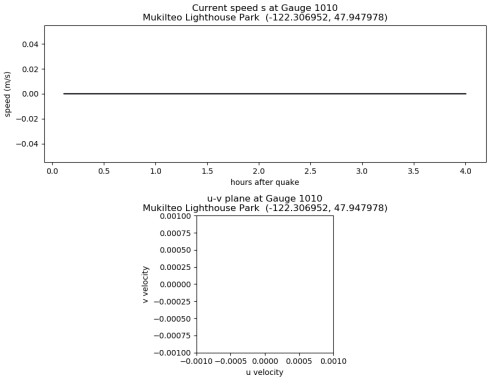

CSZ L1 event:

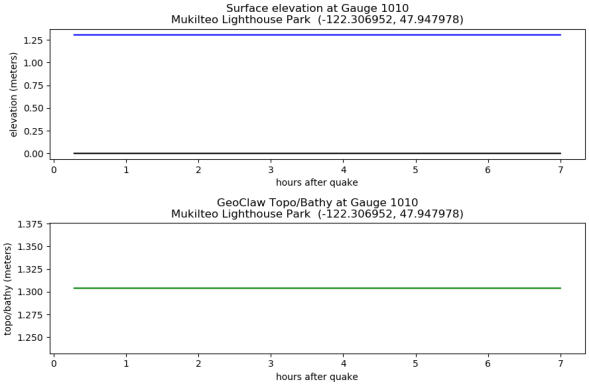

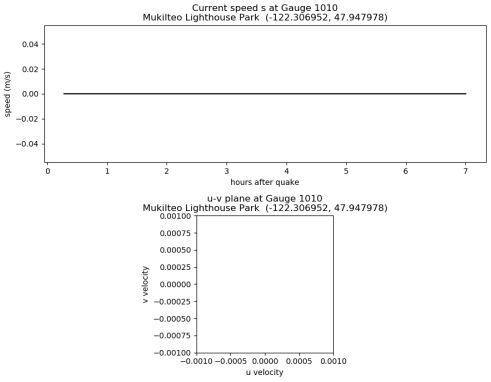

AKmaxWA event:

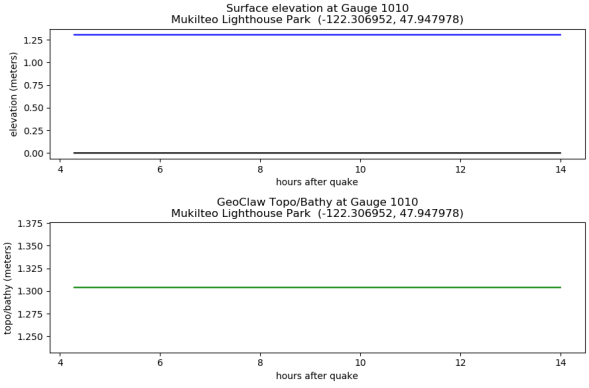

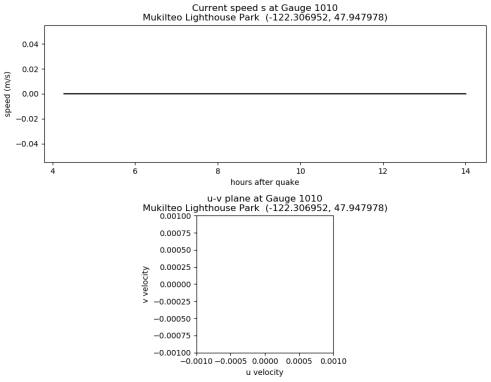

Gauge 11: Edmonds Ferry Terminal.

Computed on region `SnohoSouth`.

SF-L event:

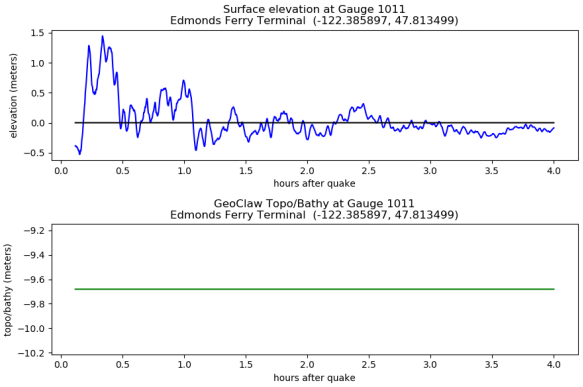

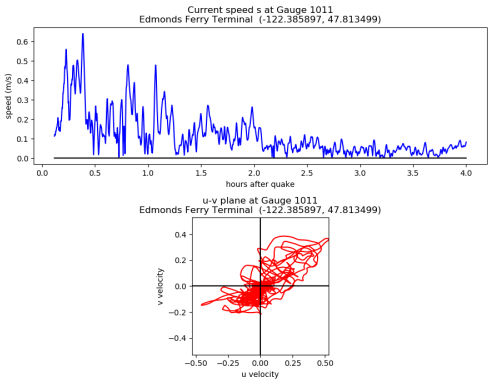

CSZ L1 event:

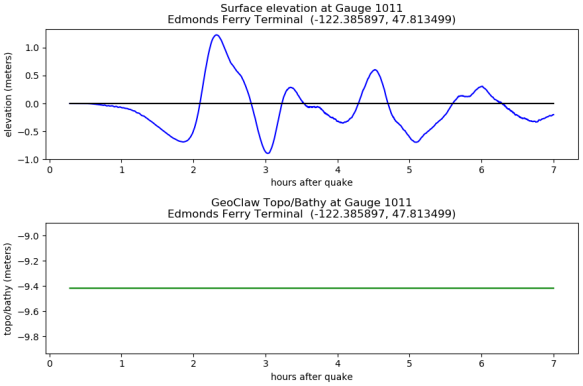

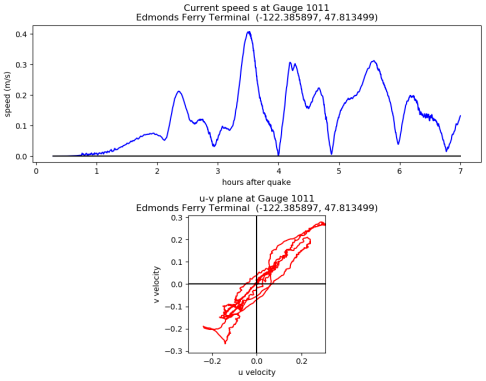

AKmaxWA event:

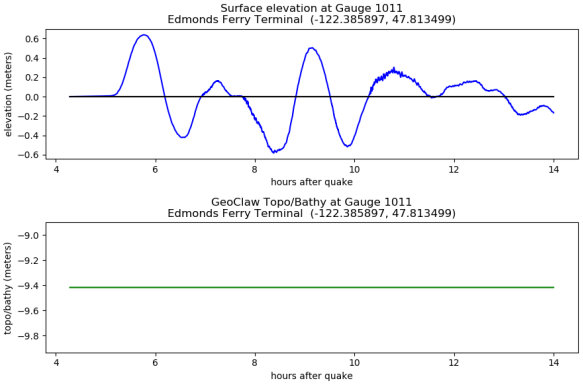

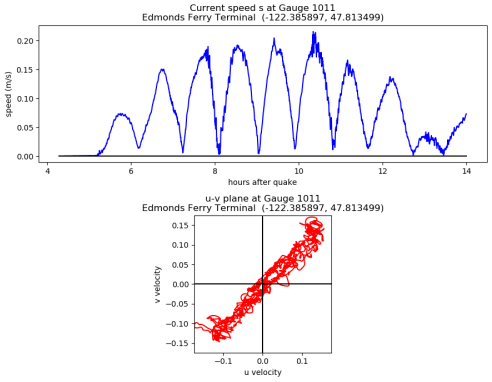

Gauge 501: South of Edmonds.

Computed on region `SnohoSouth`.

SF-L event:

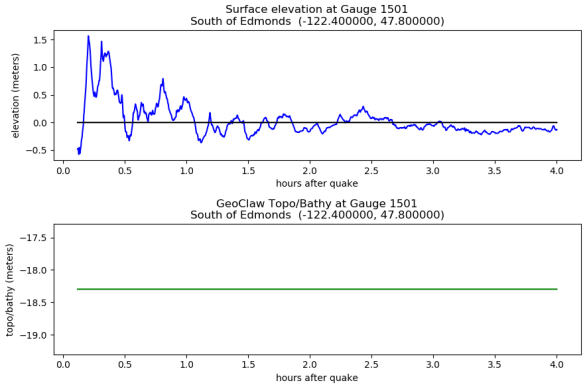

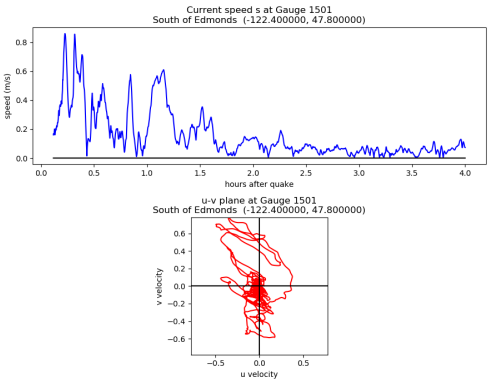

CSZ L1 event:

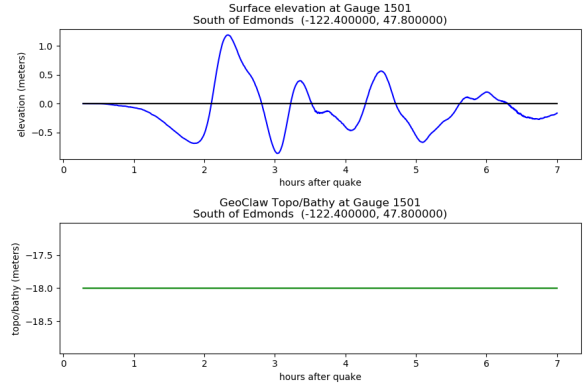

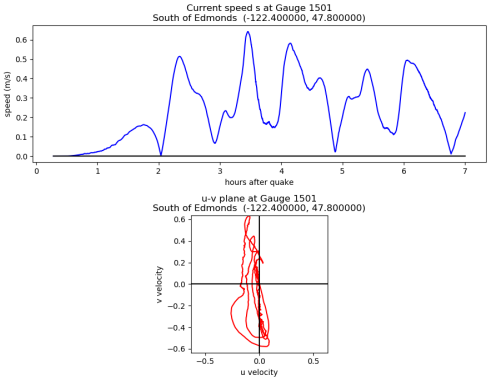

AKmaxWA event:

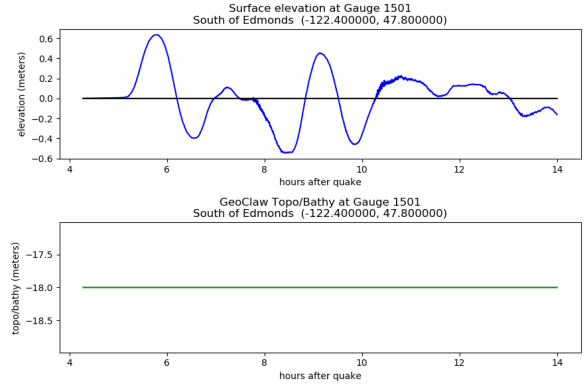

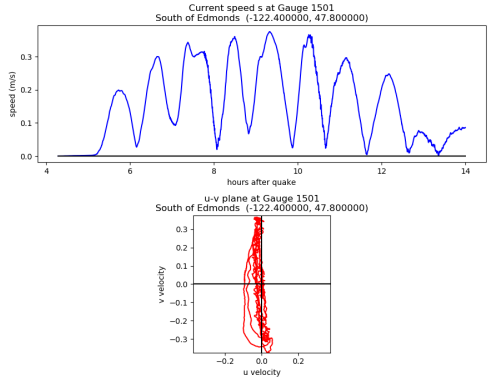

Gauge 502: SE of Cultus Bay.

Computed on region `SnohoSouth`.

SF-L event:

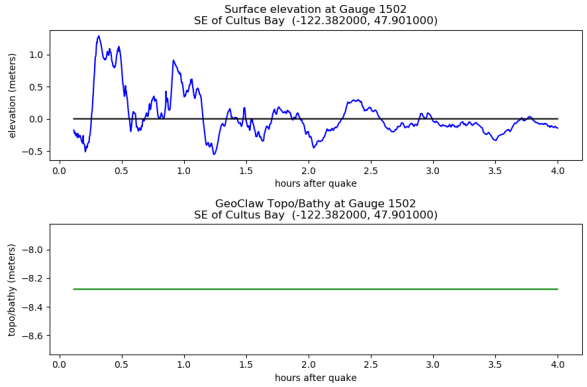

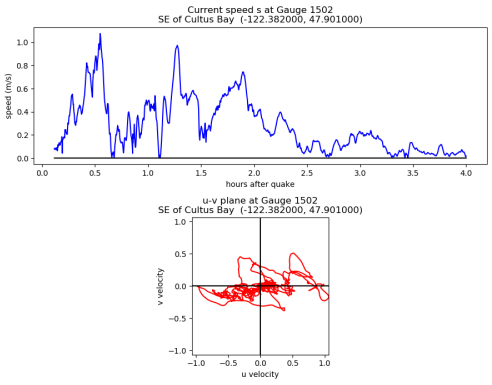

CSZ L1 event:

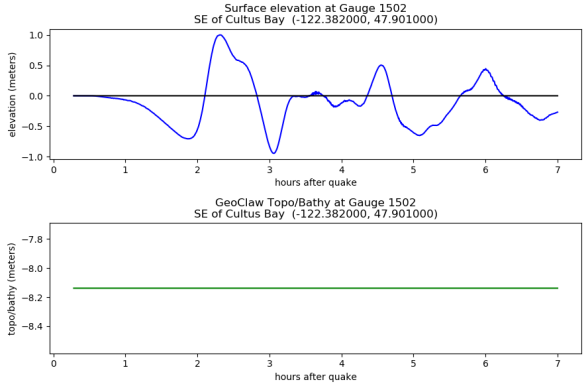

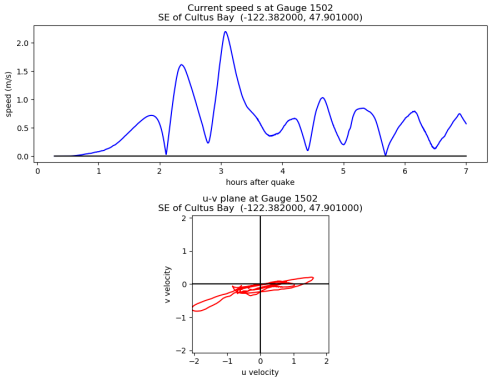

AKmaxWA event:

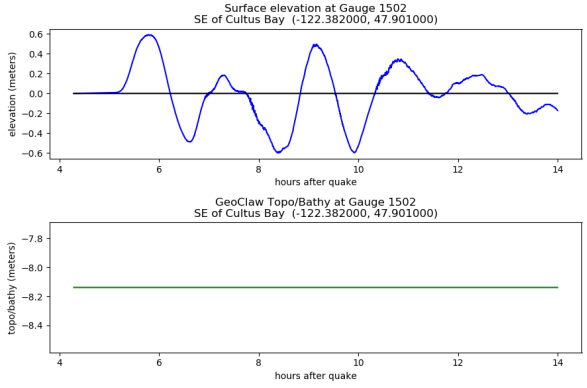

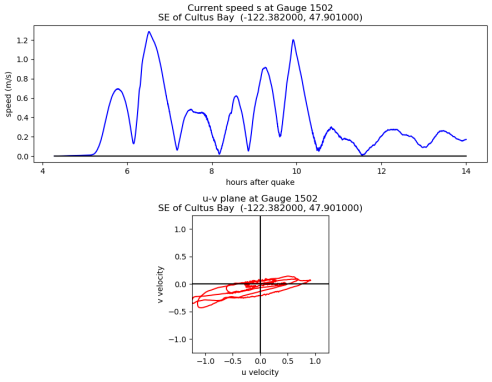

Gauge 503: Priest Point.

Computed on region `SnohoEverett`.

SF-L event:

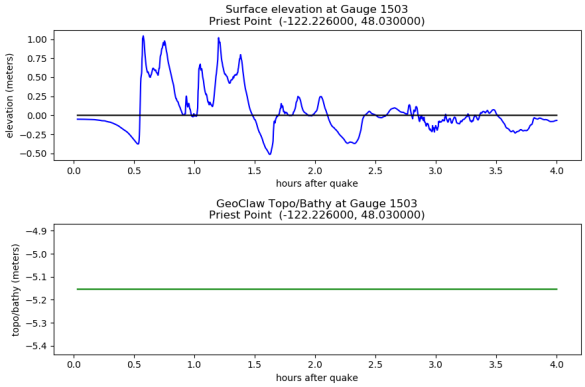

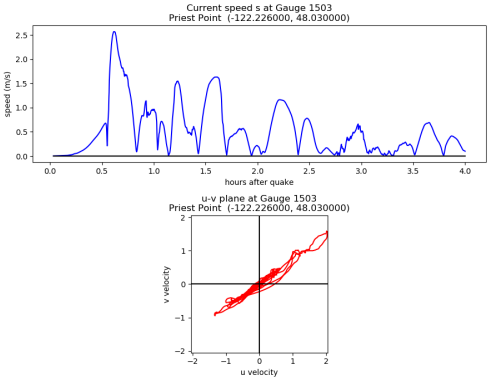

CSZ L1 event:

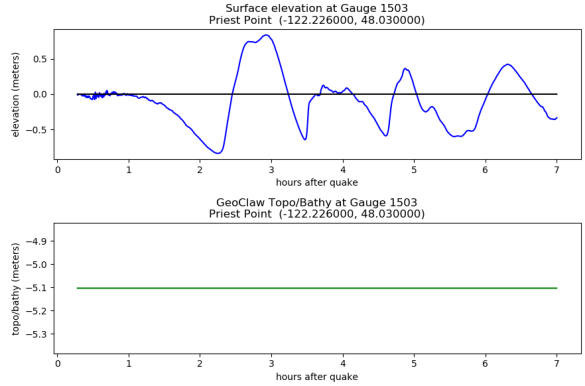

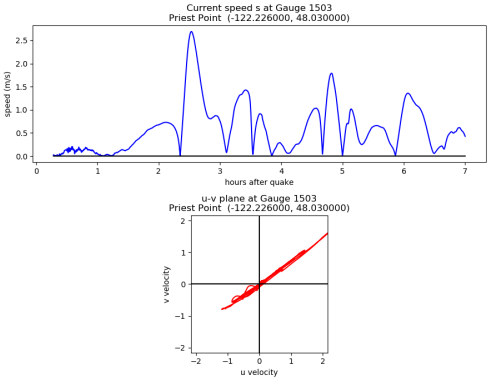

AKmaxWA event:

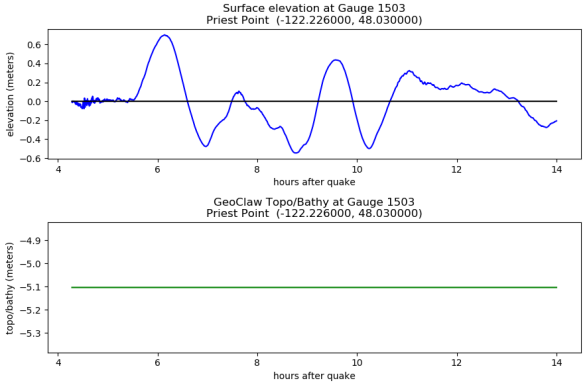

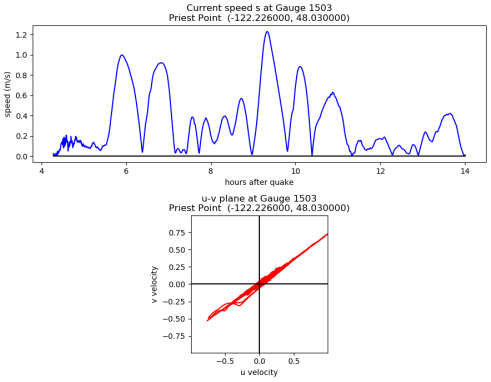

Gauge 504: Jetty Island.

Computed on region `SnohoEverett`.

SF-L event:

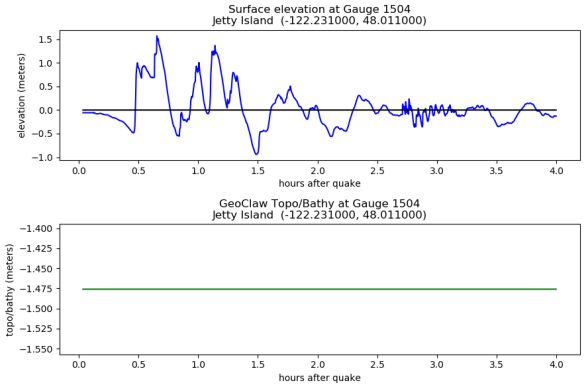

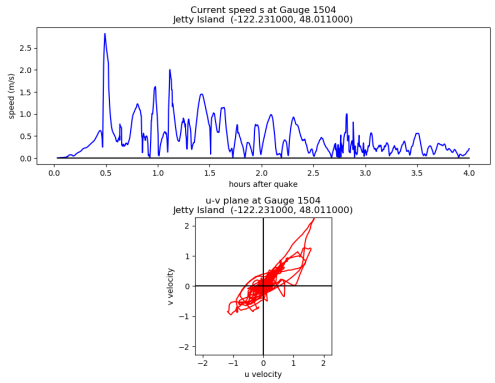

CSZ L1 event:

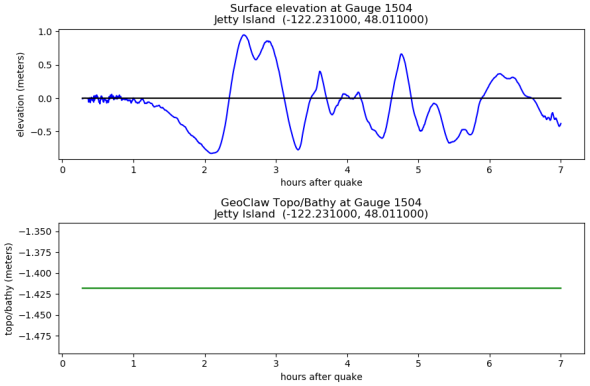

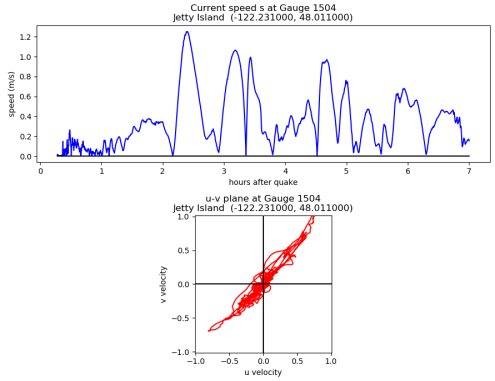

AKmaxWA event:

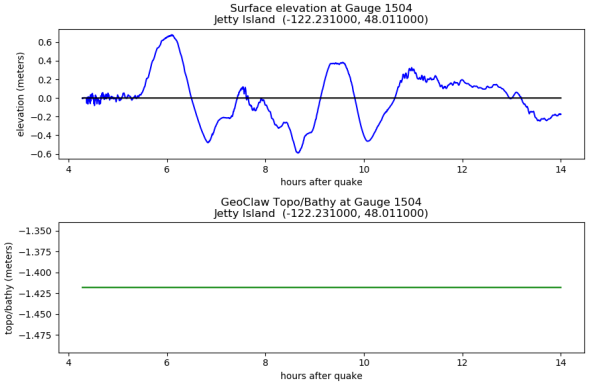

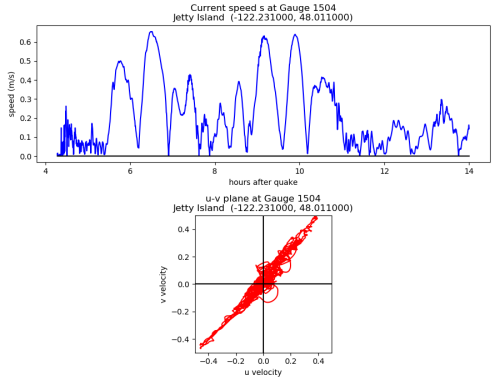

Gauge 505: SE of Hat Island.

Computed on region `SnohoSouth`.

SF-L event:

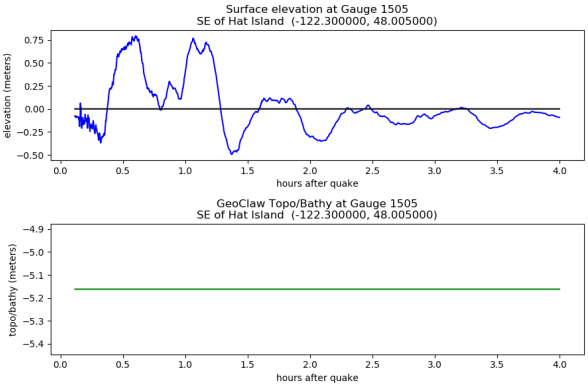

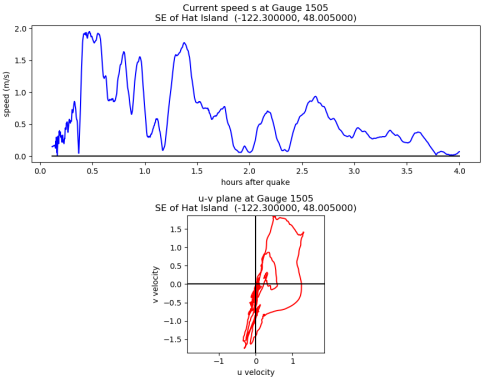

CSZ L1 event:

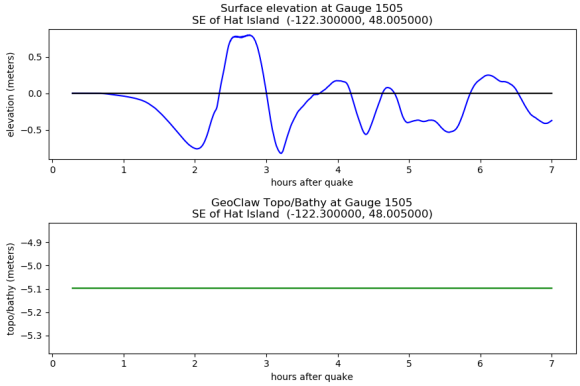

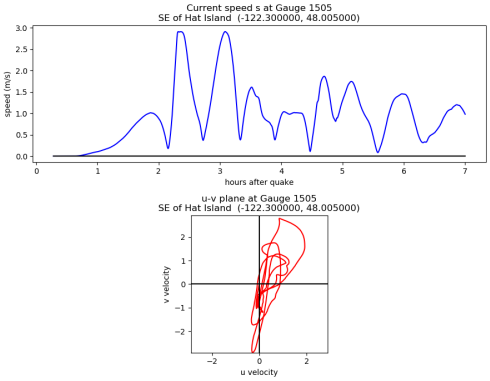

AKmaxWA event:

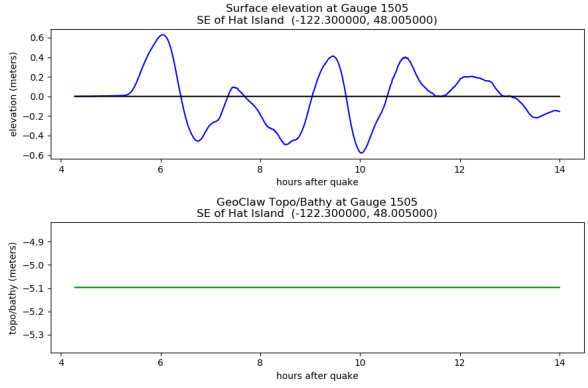

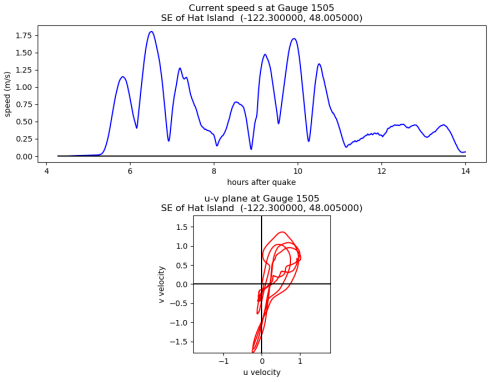

Gauge 506: SE of Camano Island.

Computed on region `SnohoSouth`.

SF-L event:

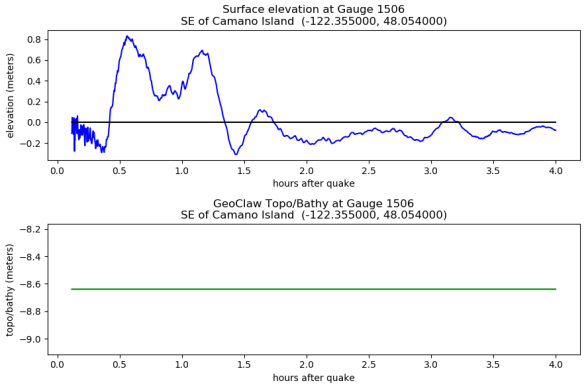

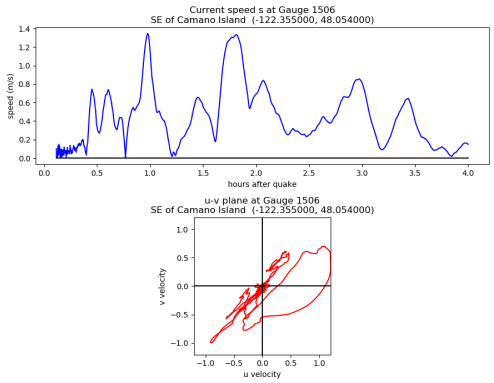

CSZ L1 event:

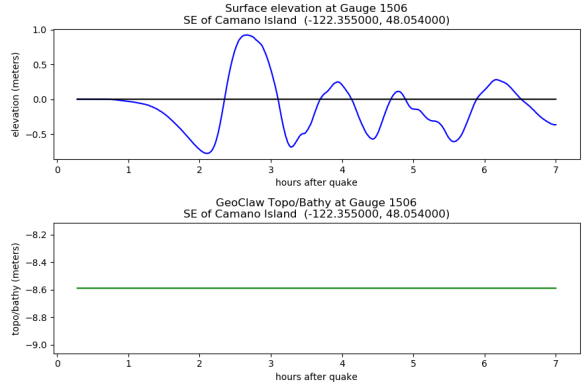

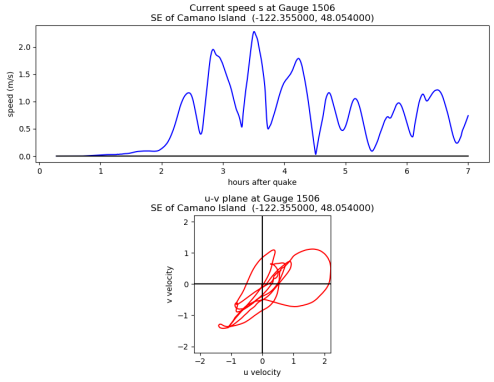

AKmaxWA event:

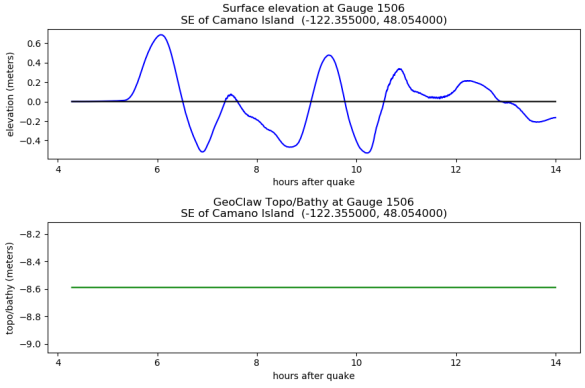

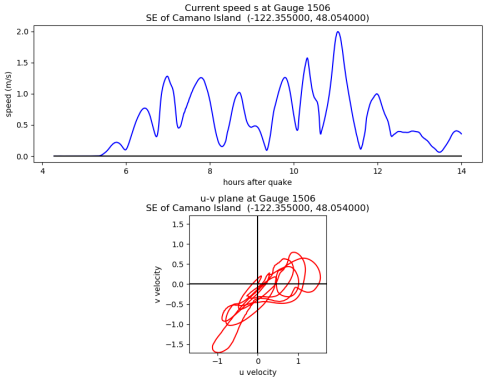

Gauge 507: Tulalip Bay.

Computed on region `SnohoSouth`.

SF-L event:

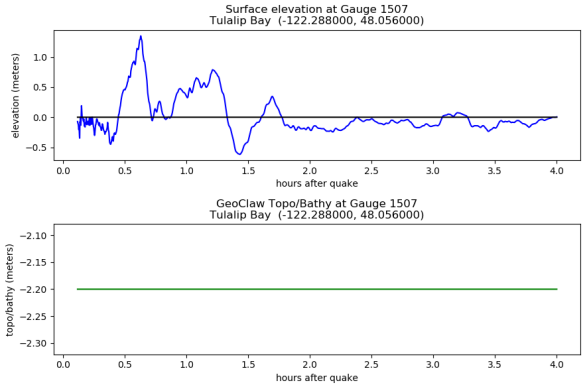

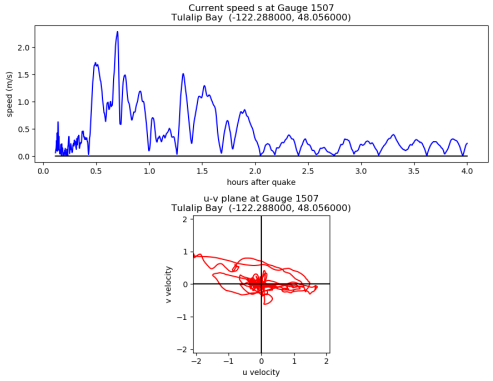

CSZ L1 event:

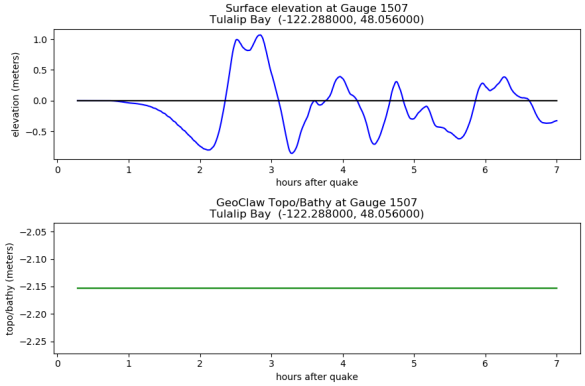

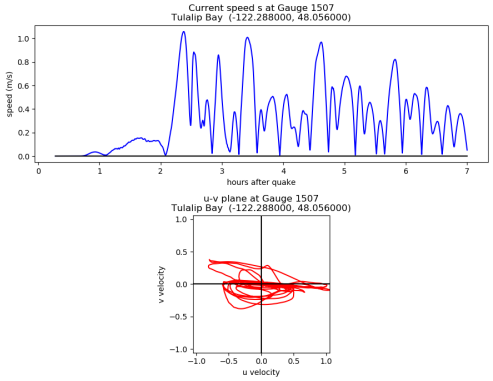

AKmaxWA event:

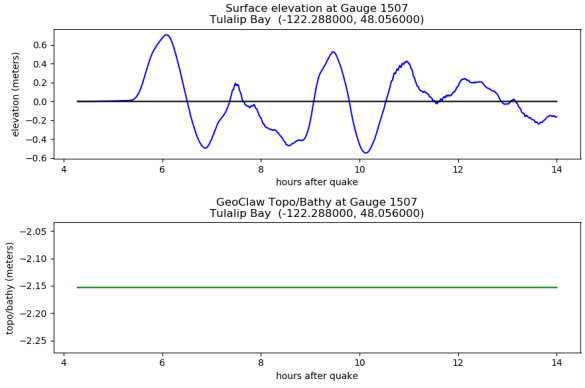

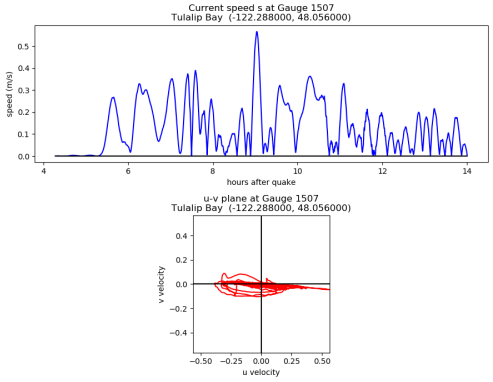

Gauge 508: Driftwood Shores Camano.

Computed on region `SnohoNorth`.

SF-L event:

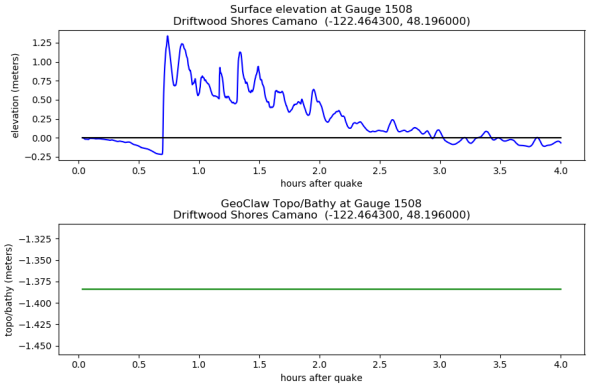

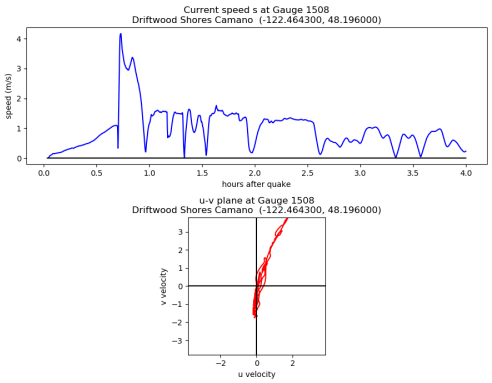

CSZ L1 event:

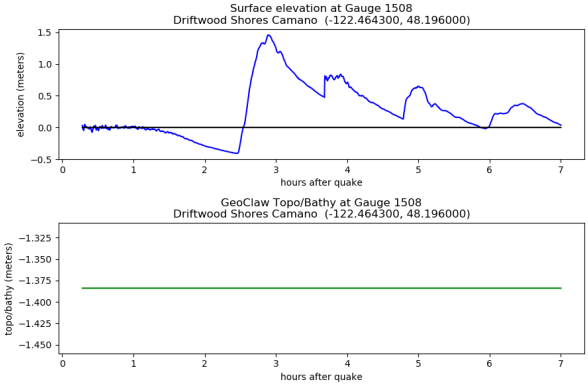

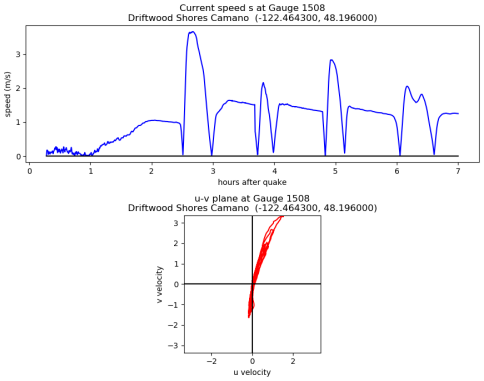

AKmaxWA event:

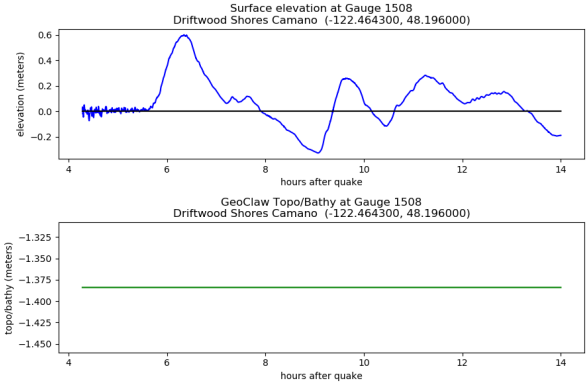

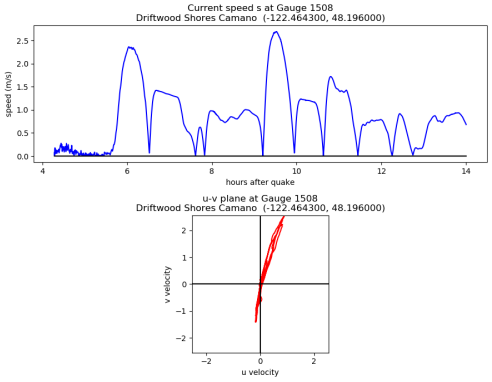

Gauge 509: Stillaguamish River outlet.

Computed on region `SnohoNorth`.

SF-L event:

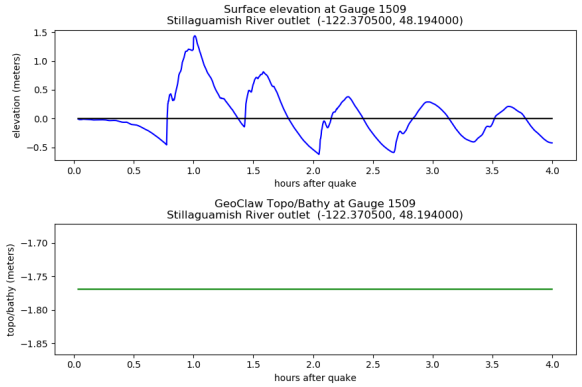

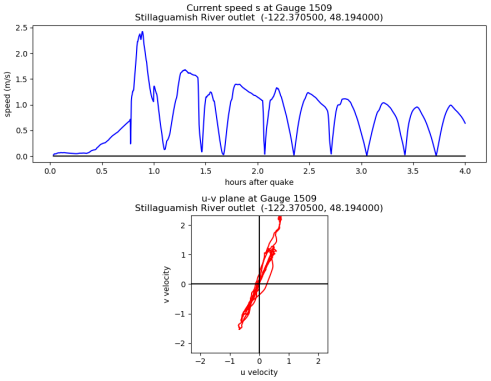

CSZ L1 event:

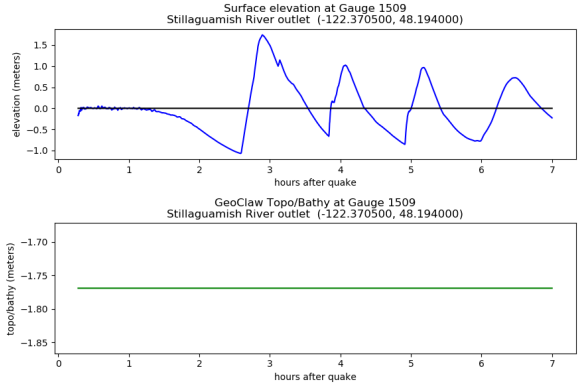

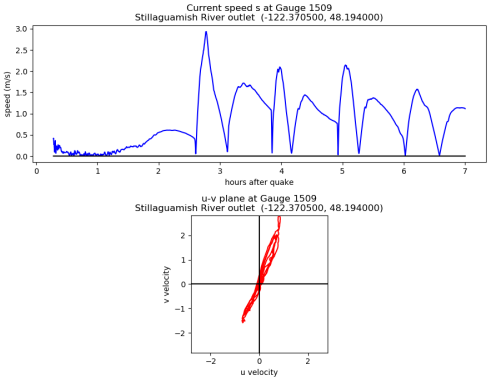

AKmaxWA event:

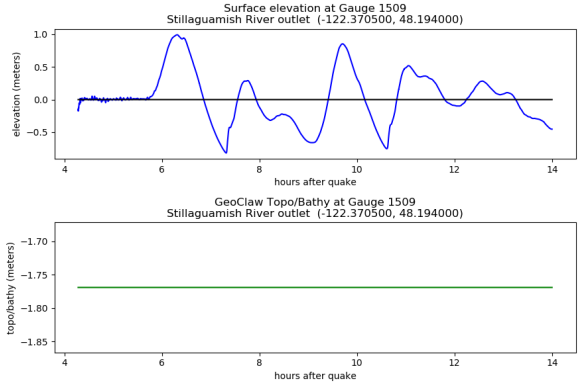

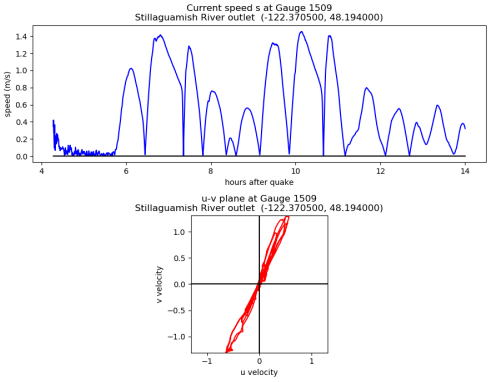

Gauge 510: Iverson Trail Camano.

Computed on region `SnohoNorth`.

SF-L event:

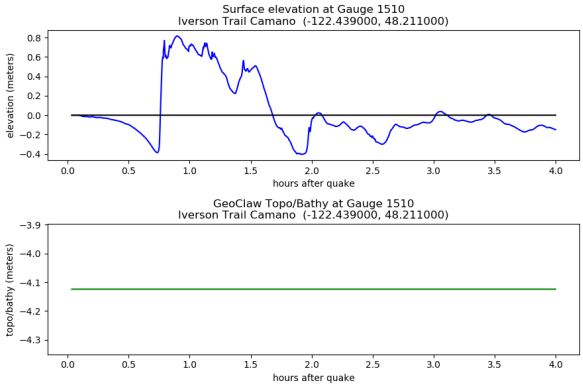

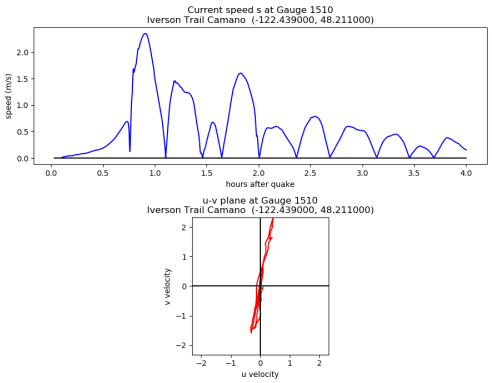

CSZ L1 event:

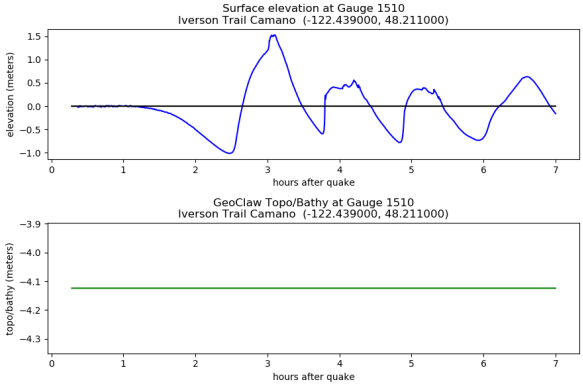

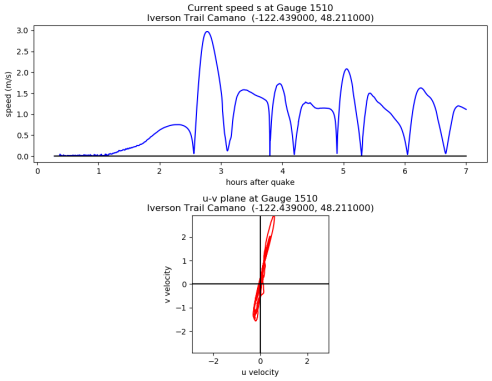

AKmaxWA event:

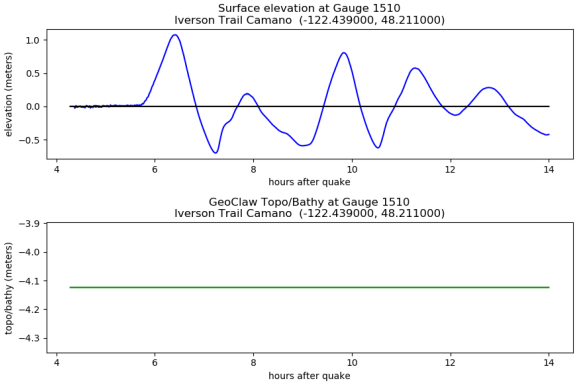

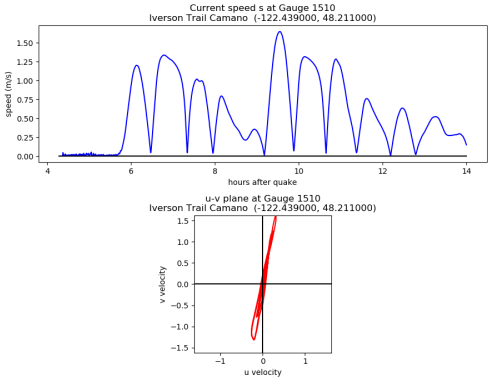

Gauge 511: Inner Cultus Bay.

Computed on region `SnohoSouth`.

SF-L event:

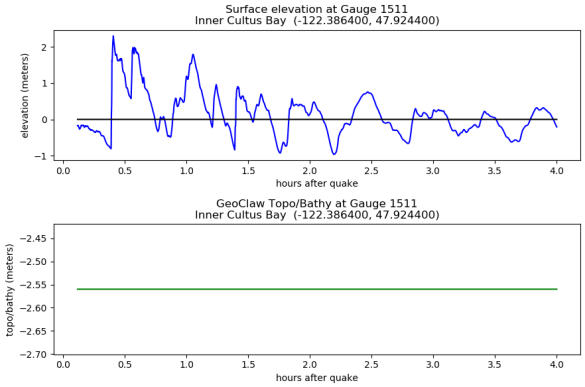

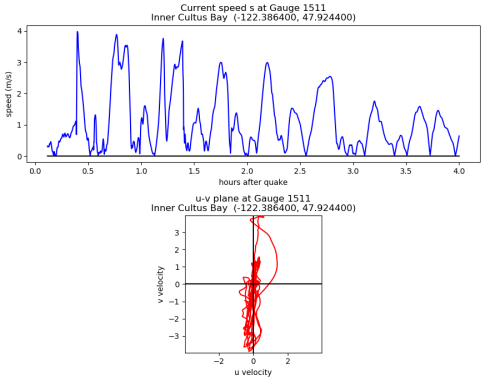

CSZ L1 event:

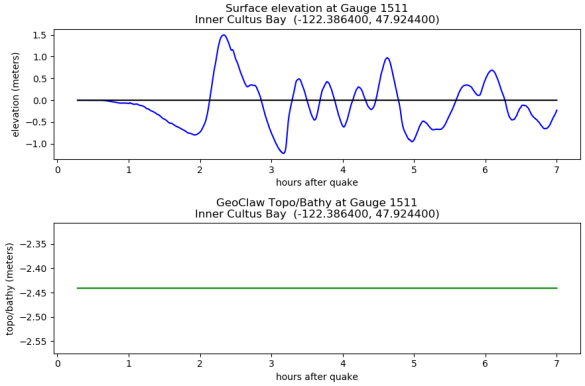

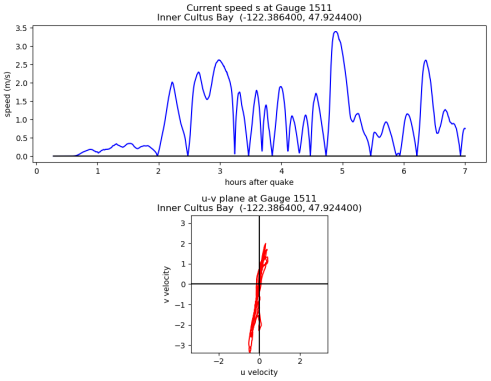

AKmaxWA event:

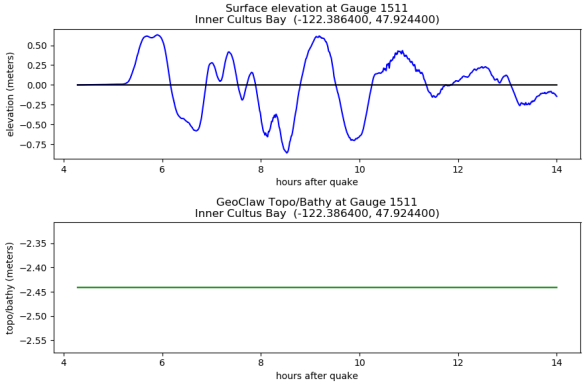

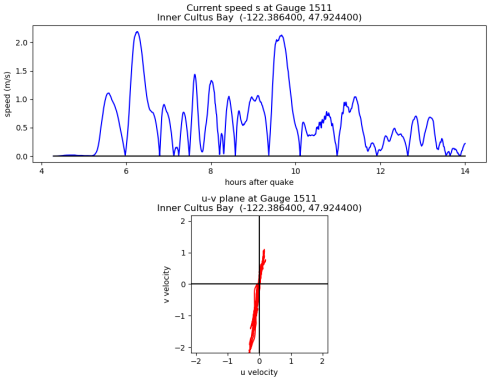

Appendices

A Data format

For each earthquake source, output data is provided in a set of netCDF files, one for each of the regions listed in Table 1 and shown in Figures 6–8. There are 3 files for each source and three sources, so a total of 9 netCDF files are provided with results. The netCDF files archived have names of the form `REGION_EVENT_results.nc` where `REGION` is replaced by the fgmax region on which it was computed, and `EVENT` is replaced by the event (one of `SFL, CSZ_L1, AK`).

The netCDF files contain the field variables described below. Some are generated before the GeoClaw run as part of the input, and are independent of the tsunami source event, depending only on the fgmax region. Others are generated after the run from the fgmax output. Note that all variables are stored on two-dimensional uniform grids as defined by the `lon` and `lat` arrays. Only the points on this grid where `fgmax_point == 1` are used as fgmax points and only at these points is fgmax output available.

Values created as part of the GeoClaw input:

`lon`: longitude, x (degrees),

`lat`: latitude, y (degrees),

`Z`: topography value Z from the DEM, relative to MHW (m),

`fgmax_point`: 1 if this point is used as an fgmax point, 0 otherwise,

`force_dry_init`: 1 if this point is forced to be dry regardless of initial topography elevation, 0 if this point is initialized as usual by filling in water to MHW.

Values created based on the GeoClaw output:

`dz`: Co-seismic surface deformation interpolated to each point (m),

`B`: post-seismic topography value B from GeoClaw at gauge location (m),

`h`: maximum depth of water over simulation (m),

`s`: maximum speed over simulation (m/s),

`hss`: maximum momentum flux hs^2 over simulation (m^3/s^2),

`hmin`: minimum depth of water over simulation (m),

`arrival_time`: apparent arrival time of tsunami (s),

In addition, the netCDF files contain the following metadata values:

`tfinal`: Final time of GeoClaw simulation (seconds),

`history`: Record of times data was added to file,

`outdir`: Location of output directory where data was found,

`run_finished`: Date and time run finished,

Recall that the fgmax points are exactly aligned with the 1/3" DEM points. The finest level computational finite volume grid is also aligned so that cell centers are exactly at the fgmax points, and Z in the netCDF file is the value from the DEM at this point. However, the topography value B used in a grid cell in GeoClaw is obtained by integrating a piecewise bilinear function that interpolates the 1/3" DEM, and so B does not exactly equal Z initially. Moreover, B is the value after any co-seismic deformation associated with the event.

A.1 Gauge time series

The gauge time series was captured from each simulation every time step, but was then interpolated to 5 second increments to create the time series stored in the netCDF file for each gauge. The gauges were generally turned on only after the finest level computational grids were introduced around the fgmax region, and so time series do not start at $t = 0$ in general. Most gauges were within some fgmax region and so the finest computational grid around the gauge had a resolution of 1/3". The time step then depends on the maximum depth over this region (since GeoClaw requires computing with a time step satisfying the CFL condition), but in general was less than 1 second.

The netCDF files archived have names of the form `REGION_EVENT_gauge00000.nc` where `REGION` is replaced by the fgmax region on which it was computed, `EVENT` is replaced by the event (one of `SFL, CSZ_L1, AK`), and `00000` is replaced by the gauge number.

The netCDF files contain the following field variables:

`times`: time (seconds post-quake),
`zGeo`: post-seismic topography value B from GeoClaw at gauge location (m),
`h`: depth of water at gauge in simulation (m),
`u`: E/W velocity u at gauge (m/s),
`v`: N/S velocity v at gauge (m/s),
`level`: AMR refinement level at gauge at this time.

In addition, the netCDF files contain the following metadata values:

`history`: Record of times data was added to file,
`outdir`: Location of output directory where data was found,
`run_finished`: Date and time run finished,

B CSZ L1 model comparisons

The comparisons shown in this section are taken from Version 1 of this report [16] and was done on 2/3" by 1/3" grids. These tests have not been redone on 1/3" by 1/3" resolution.

Figure 3 shows two different versions of the CSZ L1 deformation. To check that the choice of deformation makes little difference in the results, we ran some simulations with both versions. Figure 12 shows a comparison or results in the region denoted `lat_4795_4807` in the earlier reports, near Everett.

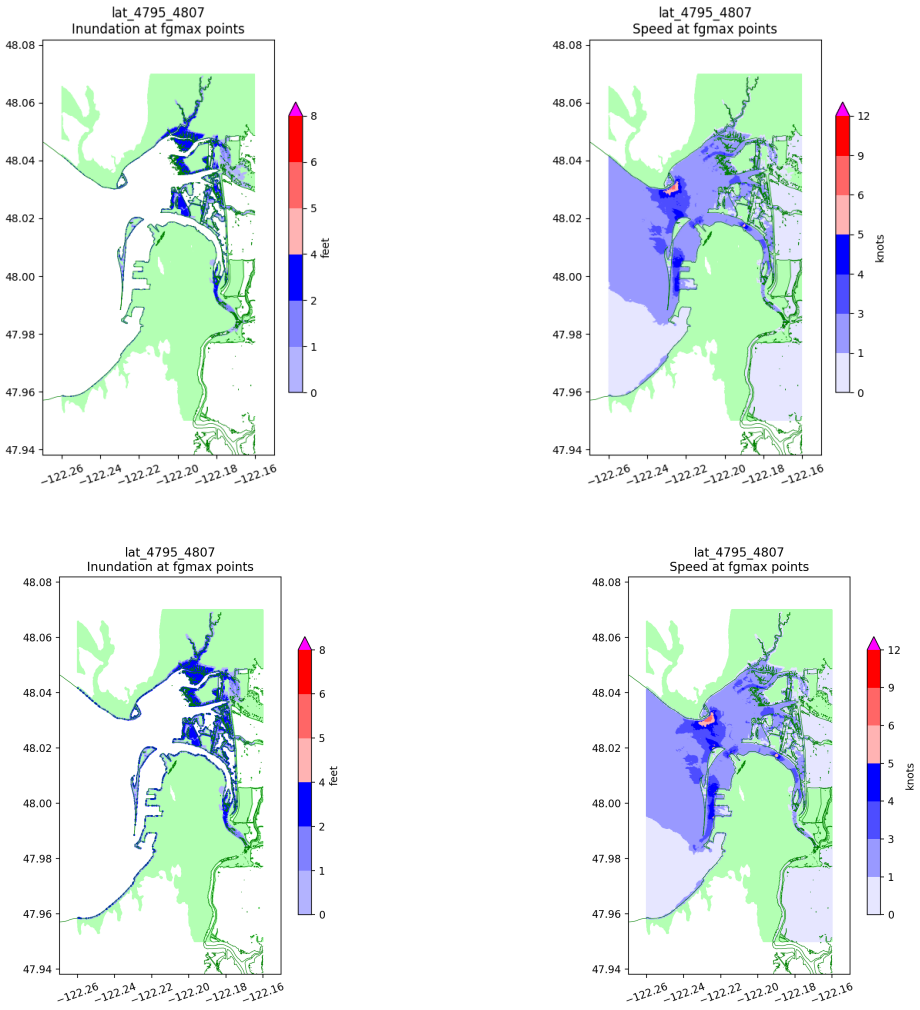

Figure 12: Results near Everett using the CSZ L1 event. The top row shows results with the version of L1 provided by PMEL, which was used to produce the published results for all regions. For comparison, the bottom row shows the results are very similar when the UW extension of L1 is used instead.

C Seattle Fault scenario issues

This appendix is unchanged from Versions 1 and 2of this report [16], [17]. Note that in subsequent work [17, 1, 29, 2] the event denoted SF-L has continued to be used, as described here. The event denoted SF-S has not been used in later studies due to the very small tsunami that is produced.

In five Seattle Fault tsunami modeling studies published during the period 2001–2015 [5, 14, 15, 30, 31], there appear to be inconsistencies in the fault plane models that were applied, perhaps due to evolving understanding of the fault structure. Koshimura et al. [14, 15] developed a fault model according to the structure inferred by [25] and [13]. In addition to these reports, guidance for development of the later models [5, 30, 31] was provided by (a) the 2002 report updating the National Seismic Hazard Maps [8], (b) a joint NOAA/USGS/WADNR/WAEMD 2002 Workshop to develop quantitative descriptions of potential tsunamigenic earthquake, landslide and delta failure events in Puget Sound [12], (c) a 2007 study of Seattle seismic hazards [9] and (d) discussions with the authors of these reports.

The 2002 Workshop focused on development of earthquake models for two Seattle Fault events described by Frankel et al. [8]; the first, an Mw > 7 magnitude with recurrence period ~ 5000 years, the second was a smaller Mw > 6.5 with recurrence of ~ 1000 years (see Table 2.1 of [12]), which we here refer to as SF-L and SF-S, respectively. In the reports cited above they are referred to as Mw 7.3 and Mw 6.7 events, but we have found in many cases that the reported values of the fault parameters produce events with different magnitudes.

C.1 The SF-L event

The SF-L event was designed to model the earthquake that occured roughly 1100 years ago, and for which geologic data is available for the uplift or subsidence at several locations, in particular Restoration point (7 m), Alki Point (4 m), and West Point (-1 m). The original tsunami source was designed by Koshimura et al. [14] based on seismic reflection data of Pratt et al. [25] and consisted of 12 subfaults, 6 shallow (≤ 5.5 km) and 6 deep (≥ 5.5 km) segments. The shallow segments dip at 60° and the deep ones at 25°. It is not clear why these dip angles were chosen, since in [25] it is stated that the fault dips at about 20°, steepening to 45° near the surface. The shallow subfaults have width 6 km and the deep ones have width 38 km. The depth of the subfaults below the surface is not given. Koshimura et al. [14] used this set of subfaults to generate surface displacement (via the Okada model) and report deformation that agreed well at the three locations mentioned above. They also performed tsunami simulations using the TUNAMI-N2 code, comparing results at Cultus Bay on Whidbey Island to observed tsunami deposits. Unfortunately, [14] does not contain all the subfault parameters needed to reproduce this deformation. In addition to the missing depth, the latitude and longitude of each subfault is not precisely specified.

Frankel et al. [8] describe an "Mmax" 7.3 earthquake on the northern trace of three faults in the Seattle Fault zone, assuming "... faults strike east-west, dip at 45 degrees, and with a 20 km seismogenic thickness ...". The model of [14] was simplified by PMEL in consultation with DNR to obtain a 6-subfault model that was used in a 2003 tsunami hazard analysis of Seattle in PMEL-124 [30] and appears in Table 1 of that report. The magnitude was scaled back from the Mw 7.6 event of [14] to what was claimed to be a Mw 7.3 event (although we find Mw 7.39). In this model the subfaults have width 20 km and dip 60°, rather than the 45° dip mentioned by Frankel et al. [8]. The depth below the surface is not specified. The 60° dip is justified as "within the uncertainly range of many recent fault models", citing ten Brink et al. [28] and other studies. Slip on these subfaults was chosen to match the observations at the three locations cited above, and compared in Table 2 of [30]. Unfortunately the latitude and longitude of each subfault is not specified in this or later PMEL reports, but we have determined the position of the top-center of each subfault from discussions with PMEL and examination of past results. Table 3 gives our estimates of these values, along with the other subfault parameters that were unchanged between studies.

Essentially the same subfault model was used in the 2007 study of Tacoma in PMEL-132 [31]. However, the width of each subfault was increased from 20 km to 35 km. This was presumably done in light of work done in the meantime that suggested the fault may extend lower than 20 km.

Although the fault width was increased, the slip on each subfault was kept the same as in Table 3. This changes the magnitude of the earthquake, which is based on the logarithm of the seismic moment, defined

by

$$Mo = \mu \sum_j W_j L_j D_j \tag{1}$$

This sum is over all subfaults j, with length L_j, width W_j, and slip displacement D_j. The rigidity (shear modulus) μ was taken to be 30 GPa in Koshimaru [14] and is not stated in later studies. If the units of W_j, L_j, D_j is meters, then Mo is in Newton-meters (Nm) and the moment magnitude is then given by

$$\text{Mw} = \frac{2}{3}(\log_{10}(Mo) - 9.05). \tag{2}$$

Koshimaru [14] used a variant of this with 9.05 replaced by 9.1, which often appears in the literature and gives a value for Mw that is smaller by 0.033. The formula (2) is considered more correct[1] and agrees with the expression $\text{Mw} = \frac{2}{3}(\log_{10}(Mo) - 10.7$ for the case when Mo is measured in dyne-cm (1 dyne-cm = 10^7 Nm). Table 4 shows the magnitude that we compute using (2) for each of the past studies cited, in the lines labelled "our result".

By increasing the fault width by a factor of 35/20 while keeping the slip the same, the magnitude of the earthquake is changed by $\frac{2}{3}\log_{10}(35/20) \approx 0.162$.

On the other hand, since the new slip is added deep in the earth relative to the original slip, this increase actually causes relatively little difference in the surface deformation (and hence in the tsunami generated).

Table 4 also shows our computation of the deformation at the three points where observations are available, compared to the values that were reported in the past PMEL studies where these values were provided. We used the version of the Okada model developed as part of GeoClaw. We cannot explain yet why we get different values than the original studies.

A further mystery is why the fault deformation shown in Figure 2 of PMEL-124 [30] seems to match the contours we compute using a fault width of 35 km rather than the width 20 km recorded in [30].

A question for future studies: Should the fault width be set back to 20 km? If it is kept at 35 km, do we now say this is a Mw 7.5 event rather than Mw 7.3? If the width should be 35 km but the goal is still to model a Mw 7.3 event, then the slip should be scaled down on this wider fault by a factor of roughly 20/35. In fact we find scaling by a factor of 0.5 gives Mw 7.35, due to use of the formula (2). This event has significantly less surface deformation than the SF-L event used in past studies since less of the slip will be near the surface. The final row in Table 4 shows these values.

Subfault	Longitude	Latitude	Length	Strike	Slip
A1	-122.7599344	47.6115777	15.2 km	87.9°	1 m
A2	-122.6165584	47.6157655	6.3 km	86.6°	1 m
A3	-122.5154909	47.6132604	8.9 km	96°	12 m
A4	-122.4397627	47.6000508	3.3 km	128.8°	11 m
A5	-122.3474066	47.5826645	11.5 km	99.3°	4 m
A6	-122.1735094	47.5847905	14.9 km	81°	1 m

Table 3: Seattle Fault SF-L. This table shows the primary parameters that seem to be unchanged between different past studies. A dip of 60° has been used for all subfaults in past studies. The longitude and latitude is for the top center of the subfault, and has been inferred from the literature. The width used varies between studies.

[1] https://earthquake.usgs.gov/learn/topics/measure.php

Study	Model parameters		Deformation			
	Width	Magnitude	Alki Pt.	Restoration Pt.	West Pt.	Max
Observations [14]			4 m	7 m	-1 ± 0.5 m	
Koshimaru [14]	vary	7.6	4.2	5.3	-0.22	
Our result	vary	7.61				
PMEL-124 [30]	20	7.3	3.9	7.1	-1.3	
Our result	20	7.39	3.52	6.66	-0.97	8.05
PMEL-132 [31]	35	7.3	3.6	7.2	-1.1	
Our result	35	7.54	3.76	6.93	-1.10	8.16
Slip halved	35	7.35	1.88	3.46	-0.55	4.08

Table 4: Seattle Fault SF-L. This table shows the observed uplift or subsidence (deformation) at three locations, as reported in [14], followed by the results from three past modeling studies. The Koshimaru results were from a model with 12 subfaults. The PMEL-124 [30] and PMEL-132 [31] studies used the same parameters from Table 3, but the subfault width was increased from 20 to 35 km. The rows labelled "our result" show the magnitude we compute from (2) and, for the latter two studies, the deformation we compute from the Okada model implemented in GeoClaw using the same parameters as in each original study. We assumed all subfaults were at a depth of 500 m (top of fault to surface). The final row shows values we obtain if the slip from Table 3 is halved on each subfault to counterbalance the increase in width.

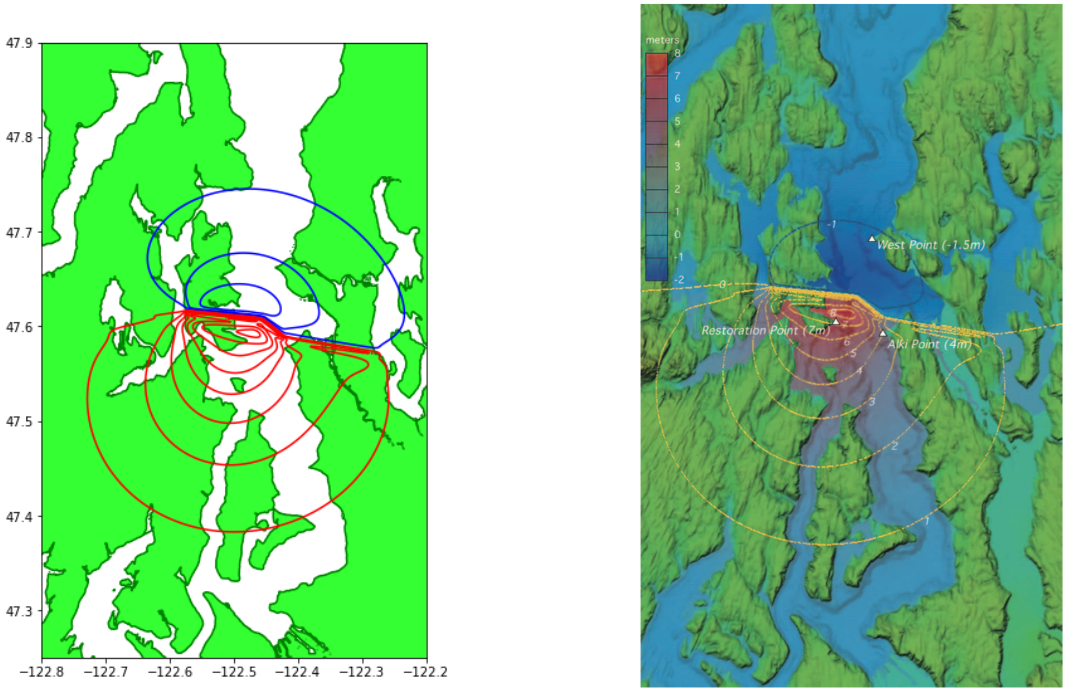

Figure 13: Left: SF-L deformation provided by PMEL and used in Snohomish County study. Right: Figure 2 from PMEL-124 [30]. Note that the contours in the figure on the right match well with those on the left and with those of Figure 14, and not so well with those shown on the left in Figure 15. This suggests a fault width of 35 km might have been used in [30], contrary to the table in that report.

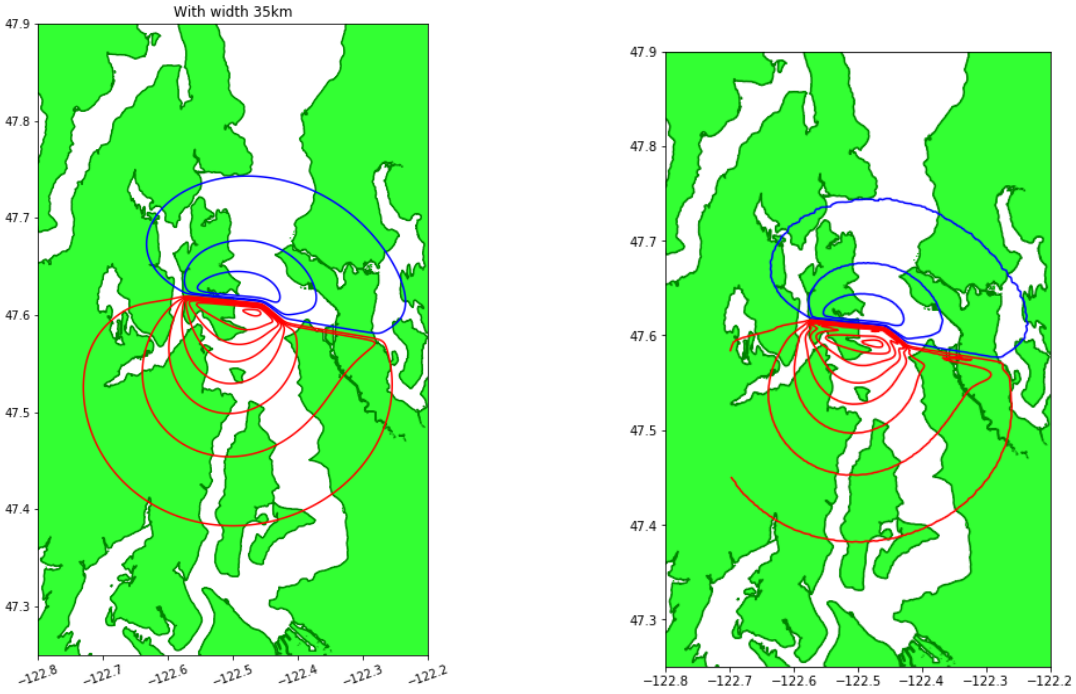

Figure 14: Left: SF-L deformation generated from subfault parameters of PMEL-124 [30], but with subfault width set to 35 km. Right: SF-L deformation provided by DNR. In both cases the red uplift contours are at increments of 1 m and the blue subsidence contours are at incrments of 0.5 m to agree with Figure 2 of [30].

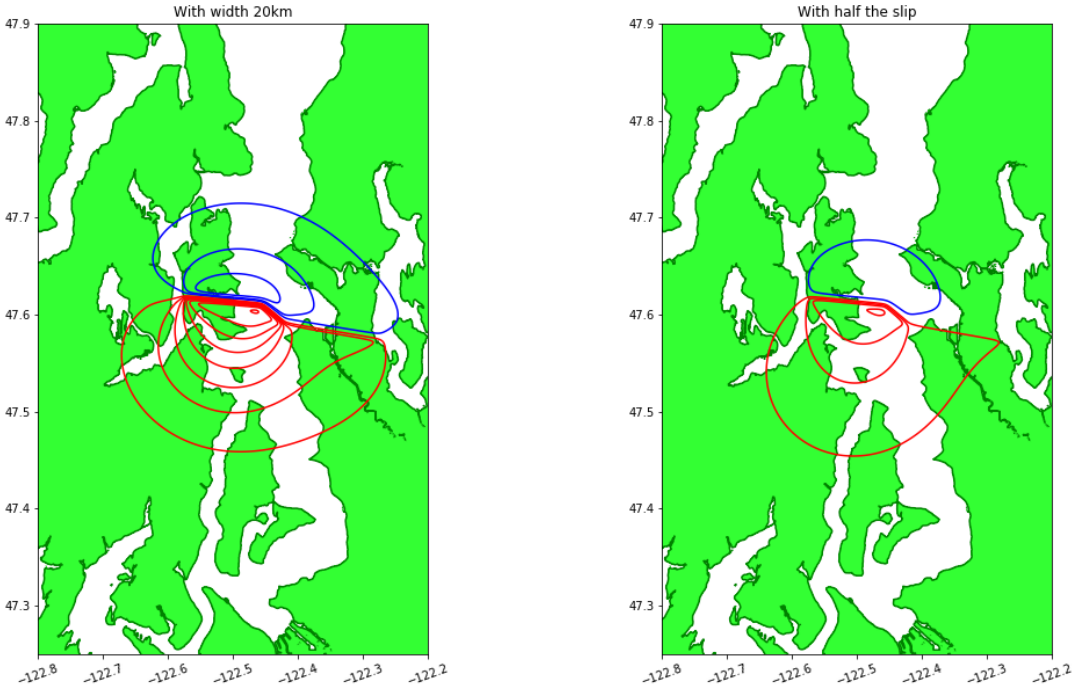

Figure 15: Left: SF-L deformation generated by setting subfault width to 20 km. Right: SF-L deformation generated by setting subfault width to 35 km but halving the slip on each subfault to recover a Mw 7.35 event.

C.2 The SF-S event

The SF-S event was used to perform some tsunami simulations in the early stages of this study. It was determined that the inundation and currents observed in Snohomish County are negligible, and so the final results provided from this study do not include SF-S simulation results.

However, in this section we collect some information about this source since several issues arose in determining the proper specification of this source based on past work. For future modeling studies where SF-S may be important, this section may prove useful.

The SF-S model was apparently first used in a PMEL study of Everett in PMEL-147 [5]. It is based on the SF-L model but is reduced to having only 4 subfaults (A2, A3, A4, and part of A5 from the SF-L subfaults of Table 3. The fault was shortened and slip values were also reduced in order to define a smaller event (claimed to be Mw 6.7) with a 50-year return time. Some of the subfault parameters are given in Table 5. The width was set to 35 km.

For reasons we do not understand, the dip was changed from 60° to 45° on all subfaults. According to Tim Walsh (personal communication), this was possibly done in order to better match observations of displacement in a trench at Vasa Park in Bellevue that might have corresponded to a Mw 6.7 type event several thousand years ago, as discussed in the EERI report [27] concerning the development of a Seattle Fault Mw 6.7 scenario. This report contains a wealth of information, but unfortunately does not give fault parameters or surface deformation in a format useful for our needs.

We also do not understand why the slip on each subfault was set to 2.8 m. According to our calculations, this gives an event with Mw 7.04, not 6.7. We find that if we instead set the slip to 1 m on each subfault, then the magnitude is Mw 6.74. Note that in the MOST input files used at PMEL the slip is set to 1 m for "unit sources" and the deformation is later scaled by the slip value. We do not know if this is related.

These parameters were taken from Table 2 of [5]. In that report there is no discussion of the depth of the subfaults, but we assume they should be the same as the SF-L scenario, where a value of 500 m (from top of fault to surface) was inferred from MOST input files provided by PMEL for SF-L.

The MOST input files provided for the SF-S event have the same parameter "htop" set to 15 km for the SF-S event. We were told that "htop" might be the distance from the *bottom* of the fault plane to the surface, but this does not make sense since with a width of 35 km and dip of 45°, the vertical distance from the top to bottom of the fault plane is $35\cos(45°) = 24$ km, and even with a dip of 60° the distance is 17.5 km, so if the bottom is at 15 km the fault would extend many km into the air. However, if the fault width were assumed to be 20 km then with dip 45° the vertical extent of the fault is 14.14 km, so setting the lower edge at 15 km would make sense. This is inconsistent with Table 2 of [5], which states the width is 35 km for each subfault.

Moreover, the plot shown in Figure 2 of [5], and the deformation files provided to us by PMEL, show a deformation that we can obtain only by placing the *top* of the fault at 15 km depth. This puts the fault much deeper than it should be and gives less surface deformation than was presumably intended. On the other hand this is counterbalanced by the increased slip and width of the fault relative to what we think was intended.

In Table 6 we present the various sets of parameters and the surface deformation at the same three locations considered using different versions of the SF-S scenario.

Figure 16 shows the surface deformation we obtain using the parameters of [5] and a depth of 15 km, and the deformation we obtain with our best guess at what the intended parameters are, which is shown in the row labelled "our best guess" of Table 6. Note that because of the cancellation of effects the maximum deformation is similar in these two plots, but the shape is very different. Moving the fault to 15 km depth gives much a more diffuse effect at the surface.

Another mystery arises when trying to reconcile the deformations we compute from the fault parameters to the deformation files provided to us by PMEL and DNR, both of which should be for this scenario but do not agree with each other or with any of the deformations we generated. PMEL provided 4 deformation files used by MOST, one for each subfault. Adding them up gives the deformation shown on the left in Figure 17. DNR provided `B_seafaultEERI/everett_b_deformation.asc` in NAD83 Washington State Plane North coordinates with horizontal units in feet (but vertical units in meters, apparently). Converting this to WGS84 latitude-longitude coordinates gives the plot shown on the right in Figure 17. The 0.5 m contour in this plot agrees quite well with the corresponding contour in Figure 2(b) of PMEL-147 [5].

For modeling Snohomish County, the differences in these deformations makes little difference because in any case the tsunami is very small, with minimal flooding and current velocities below 1 m/s almost

everywhere (see Figure 18). For the upcoming study of Bainbridge Island, it may be more important to decide on the right version of SF-S to use.

Subfault	Longitude	Latitude	Length	Strike	Slip
B1	-122.6165584	47.6157655	6.3 km	86.6°	2.8 m
B2	-122.5154909	47.6132604	8.9 km	96°	2.8 m
B3	-122.4397627	47.6000508	3.3 km	128.8°	2.8 m
B4	-122.384815	47.5868088	5.8 km	99.3°	2.8 m

Table 5: Seattle Fault SF-S. This table shows the primary parameters for the subfaults of Table 2 in [5]. A width of 35 km and dip of 45° has been used for all subfaults in [5]. The longitude and latitude is for the top center of the subfault, and has been inferred from the literature. Note that B1–B3 correspond to A2–A4 of Table 3 while B4 is a shortened version of A5, with the top center coordinates adjusted accordingly.

Source	Model parameters					Deformation			
	Width	Dip	Depth	Slip	Magnitude	Alki Pt.	Rest. Pt.	West Pt.	Max
PMEL-147 [5]	35	45	15	2.8	7.2	0.61	0.67	0.28	0.72
w/modified depth	35	45	0.5	2.8	7.2	1.47	1.85	−0.14	2.03
+modified width	20	45	0.5	2.8	7.04	1.39	1.76	−0.13	1.99
Our best guess	20	60	0.5	1.0	6.74	0.52	0.61	-0.10	0.70
MOST Deform.	?	?	?	?	?	0.21	0.23	0.20	0.24
DNR Deform.	?	?	?	?	?	0.59	0.65	0.55	0.68

Table 6: Seattle Fault SF-S. This table shows the observed uplift or subsidence (deformation) at three locations, as well as the maximum uplift. The first three rows show the original values from PMEL-147, with the depth moved to 0.5 km, and with the width also reduced from 35 to 20 km. "Our best guess" is the values we think were originally intended. The MOST deformation file was provided by PMEL and the DNR deformation file was provided by DNR, both supposedly were what was used in the PMEL-147 study.

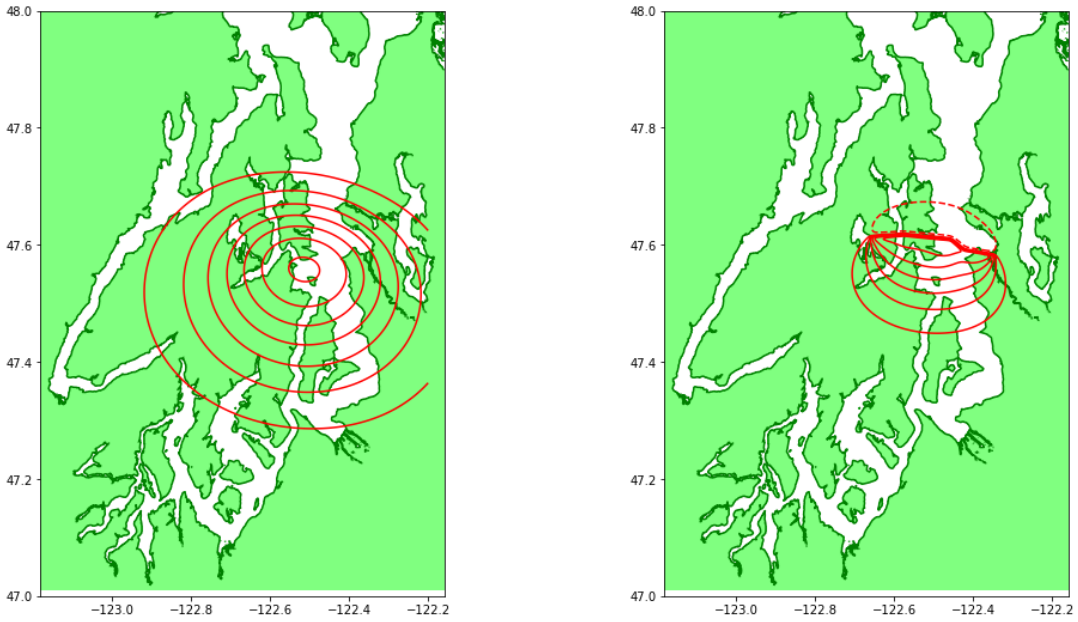

Figure 16: Left: Deformation generated with fault parameters specified in PMEL-147 [5] and with the depth set to 15 km at the top of the fault. Maximum uplift is 0.72 m. Right: Deformation generated with our best guess at the intended fault parameters, the row in Table 6 labelled "our best guess". Maximum uplift is 0.70 m. In both cases the contours are at increments of 0.1 m.

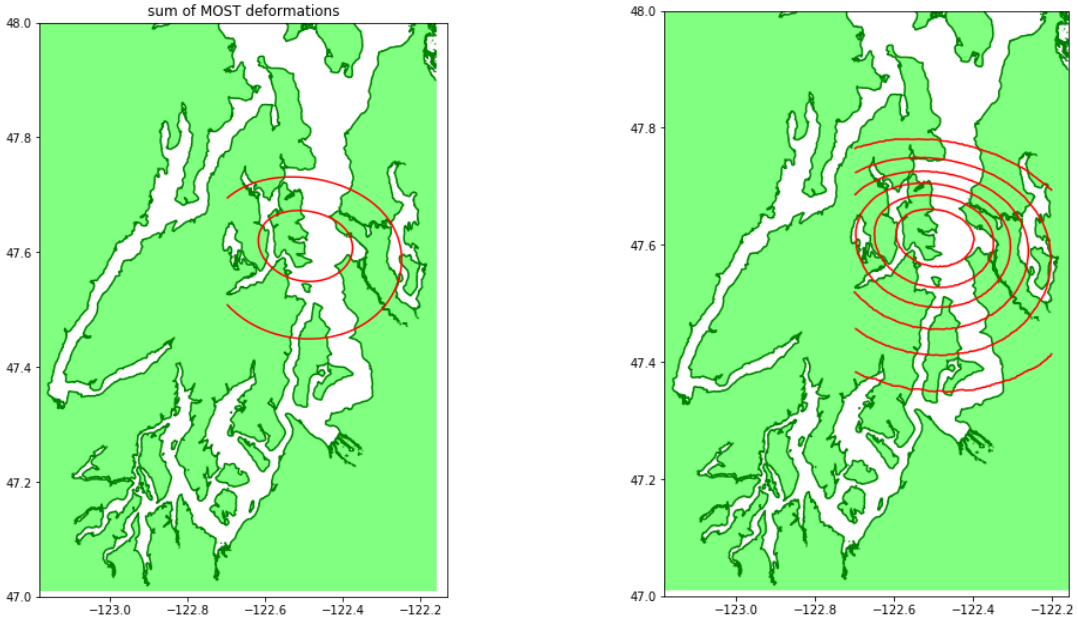

Figure 17: Left: Deformation provided by PMEL from MOST input files. Maximum uplift is 0.24 m. Right: Deformation provided by DNR as `B_seafaultEERI`. Maximum uplift is 0.68 m. In both cases the contours are at increments of 0.1 m.

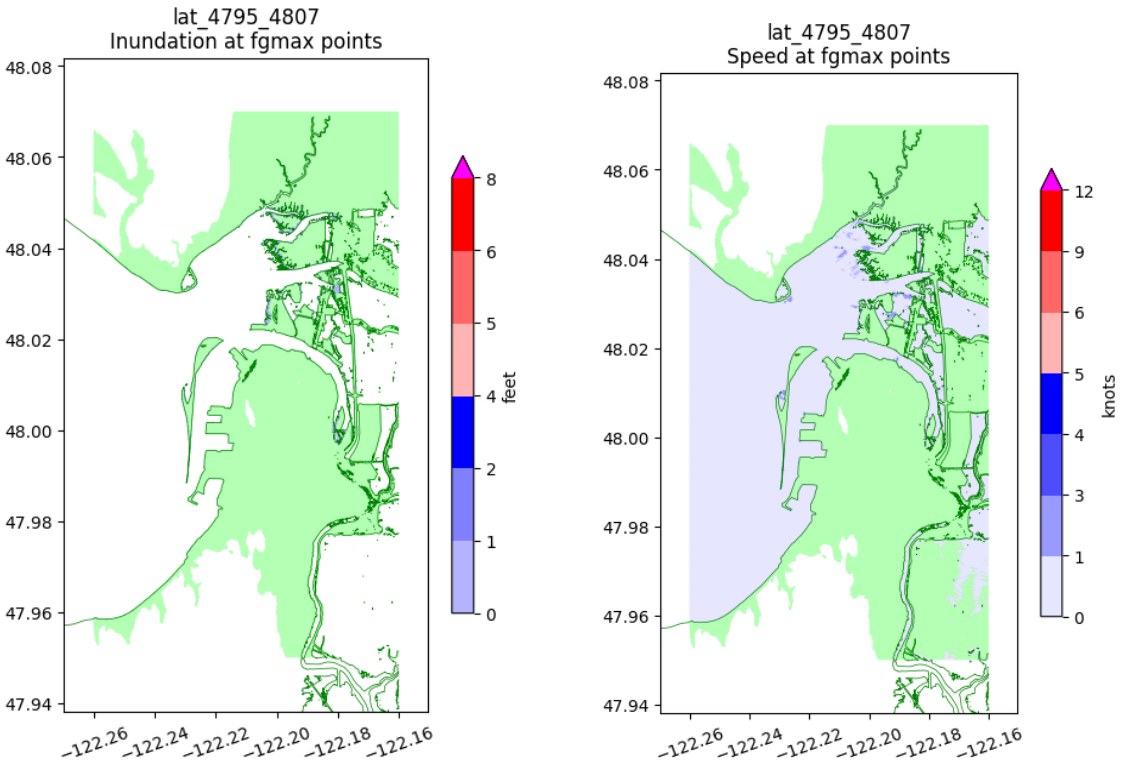

Figure 18: Maximum flow depth (left) and speed (right) calculated near Everett using our best guess at the proper SF-S model, showing no inundation and very small speeds.

Acknowledgments

The earthquake deformation files for the CSZ-L1 and SF-L events were provided by the NOAA Center for Tsunami Research (NCTR), PMEL. We acknowledge computing time provided by the CU-CSDMS High-Performance Computing Cluster, and by the Applied Mathematics Department at the University of Washington. We thank NCEI for providing the merged 1/3" DEM and the new 1/9" tiles covering Everett and the Snohomish River Valley.

References

[1] L. Adams, F. González, and R. LeVeque, *Tsunami Hazard Assessment of Whatcom County, Washington, Project Report – Version 2*, 2019, http://staff.washington.edu/rjl/pubs/THA_Whatcom.

[2] L. Adams, F. González, and R. LeVeque, *Tsunami Hazard Assessment of Island and Skagit Counties Washington, Project Report*, 2020, http://staff.washington.edu/rjl/pubs/THA_IslandSkagit.

[3] B. Atwater, M.-R. Satoko, K. Satake, T. Yoshinobu, U. Kazue, and D. Yamaguchi. USGS professional paper 1707, 2005.

[4] M. J. Berger, D. L. George, R. J. LeVeque, and K. T. Mandli, *The geoclaw software for depth-averaged flows with adaptive refinement.* Preprint and simulations: www.clawpack.org/links/papers/awr10, 2010.

[5] C. Chamberlain and D. Arcas, *Modeling tsunami inundation for hazard mapping at Everett, Washington, from the Seattle Fault.* OAA Technical Memorandum OAR PMEL-147, 2015, https://doi.org/10.7289/V59Z92V0, https://repository.library.noaa.gov/view/noaa/11189.

[6] C. D. Chamberlain, V. V. Titov, and D. Arcas, *Modeling tsunami inundation impact on the Washington coast from distant seismic sources.* PMEL Tech report, 2009, ??

[7] Clawpack Development Team, *Clawpack software*, 2017, https://doi.org/10.5281/zenodo.820730, http://www.clawpack.org. Version 5.4.1.

[8] A. D. Frankel, M. D. Petersen, C. S. Mueller, K. M. Haller, R. L. Wheeler, E. V. Leyendecker, R. L. Wesson, et al., *Documentation for the 2002 update of the national seismic hazard maps.* U.S. Geological Survey Open-File Report 02-420, 2002, http://geohazards.cr.usgs.gov/eq/of02-420/OFR02-420.pdf.

[9] A. D. Frankel, W. J. Stephenson, D. L. Carver, et al., *Seismic Hazard Maps for Seattle, Washington, Incorporating 3D Sedimentary Basin Effects, Nonlinear Site Response, and Rupture Directivity.* ?, 2007.

[10] C. Garrison-Laney, *A comparison of L1 and similar Cascadia earthquake sources used in Washington State tsunami modeling.* Available on request, 2017.

[11] F. González, R. J. LeVeque, J. Varkovitzky, P. Chamberlain, B. Hirai, and D. L. George, *GeoClaw Results for the NTHMP Tsunami Benchmark Problems.* http://depts.washington.edu/clawpack/links/nthmp-benchmarks/geoclaw-results.pdf, 2011.

[12] F. González, B. Sherrod, B. Atwater, A. Frankel, S. Palmer, et al., *2002 Puget Sound Tsunami Sources Workshop Report. A contribution to the Inundation Mapping Project of the U.S. National Tsunami Hazard Mitigation Program.* NOAA OAR Special Report, 2003.

[13] S. Y. Johnson, S. V. Dadisman, J. R. Childs, and W. D. Stanley, *Active tectonics of the seattle fault and central puget sound, washingtonimplications for earthquake hazards*, Geol. Soc. Amer. Bull., 111 (1999), pp. 1042–1053, https://doi.org/10.1130/0016-7606.

[14] S. Koshimura, H. O. Mofjeld, F. I. González, and A. L. Moore, *Modeling the 1100 bp paleotsunami in Puget Sound, Washington*, Geophysical Research Letters, 29 (2002), p. 1948, https://doi.org/10.1029/2002GL015170, http://onlinelibrary.wiley.com/doi/10.1029/2002GL015170/abstract.

[15] S. Koshimura, A. L. Moore, and H. O. Mofjeld, *Simulation of paleotsunamis in Puget Sound, Washington*, in International Tsunami Symposium 2001 Proceedings, ?, ed., vol. ? of ?, ?, 2001, pp. 761–773.

[16] R. LeVeque, F. González, and L. Adams, *Tsunami Hazard Assessment of Snohomish County, Washington, Project Report – Version 1*, 2017, http://staff.washington.edu/rjl/pubs/THA_Snohomish.

[17] R. LeVeque, F. González, and L. Adams, *Tsunami Hazard Assessment of Snohomish County, Washington, Project Report – Version 2*, 2018, http://staff.washington.edu/rjl/pubs/THA_Snohomish.

[18] R. J. LeVeque, D. L. George, and M. J. Berger, *Tsunami modeling with adaptively refined finite volume methods*, Acta Numerica, (2011), pp. 211–289.

[19] R. J. LeVeque, F. I. González, and L. M. Adams, *Tsunami Hazard Assessment of Snohomish County, Washington.* (website containing reports and data), 2018, http://depts.washington.edu/ptha/WA_EMD_Snohomish/.

[20] R. J. LeVeque, F. I. González, and L. M. Adams, *Tsunami Hazard Assessment of Snohomish County, Washington.* (website containing reports and data), 2020, http://depts.washington.edu/ptha/WA_EMD_Snoho2/.

[21] NOAA NCEI, *Port Townsend 1/3 Arc-second MHW Coastal Digital Elevation Model.* https://www.ngdc.noaa.gov/metaview/page?xml=NOAA/NESDIS/NGDC/MGG/DEM/iso/xml/366.xml&view=getDataView&header=none, Accessed 2017.

[22] NOAA NCEI, *Puget Sound 1/3 Arc-second MHW Coastal Digital Elevation Model.* https://www.ngdc.noaa.gov/metaview/page?xml=NOAA/NESDIS/NGDC/MGG/DEM/iso/xml/5164.xml&view=getDataView&header=none, Accessed 2017.

[23] NOAA NCEI, *Strait of Juan de Fuca 1/3 arc-second NAVD 88 Coastal Digital Elevation Model.* https://www.ngdc.noaa.gov/metaview/page?xml=NOAA/NESDIS/NGDC/MGG/DEM/iso/xml/11514.xml&view=getDataView&header=none, Accessed 2017.

[24] M. D. Petersen, C. H. Cramer, and A. D. Frankel, *Simulations of Seismic Hazard for the Pacific Northwest of the United States from Earthquakes Associated with the Cascadia Subduction Zone*, Pure Appl. Geophys., 159 (2002), pp. 2147–2168.

[25] T. L. Pratt, S. Johnson, C. Potter, W. Stephenson, and C. Finn, *Seismic reflection images beneath Puget Sound, western Washington State: The Puget Lowland thrust sheet hypothesis*, Journal of Geophysical Research: Solid Earth, 102 (1997), pp. 27469–27489, https://doi.org/10.1029/97JB01830, http://onlinelibrary.wiley.com/doi/10.1029/97JB01830/abstract.

[26] K. Satake, K. Wang, and B. F. Atwater, *Fault slip and seismic moment of the 1700 Cascadia earthquake inferred from Japanese tsunami descriptions*, J. Geophys. Res., 108(B11) (2003), p. 2535, https://doi.org/10.1029/2003JB002521.

[27] M. Stewart et al., *Scenario for a Magnitude 6.7 Earthquake on the Seattle Fault.* Earthquake Engineering Research Institute and Washington Military Department, Emergency Management Division, 2015, https://www.eeri.org/projects/earthquake-scenarios/seattle-fault-scenario/.

[28] U. S. ten Brink, P. C. Molzer, M. A. Fisher, et al., *Subsurface geometry and evolution of the Seattle fault zone and the Seattle basin, Washington*, Bull. Seismol. Soc. Am., 92 (2002), pp. 1737–1753.

[29] V. Titov, D. Arcas, C. Moore, R. LeVeque, L. Adams, and F. González, *Tsunami Hazard Assessment of Bainbridge Island, Washington, Project Report*, 2018, http://staff.washington.edu/rjl/pubs/THA_Bainbridge.

[30] V. V. Titov, F. I. González, H. O. Mofjeld, and A. J. Venturato, *NOAA TIME Seattle tsunami mapping project: procedures, data sources, and products.* NOAA Technical Memorandum OAR PMEL-124, 2003, https://repository.library.noaa.gov/view/noaa/11033.

[31] A. J. Venturato, D. Arcas, V. V. Titov, H. O. Mofjeld, C. C. Chamberlain, and F. I. González, *Modeling tsunami inundation for hazard mapping at Everett, Washington, from the Seattle Fault.* NOAA Technical Memorandum OAR PMEL-132, 2007, https://repository.library.noaa.gov/view/noaa/11070.

[32] Washington State EMD, *Modeling a Magnitude 7.4 Earthquake on the Southern Whidbey Island Fault Zone.* https://mil.wa.gov/uploads/pdf/seismic-safety-committee/whidbey%20island%20fault%20zone.pdf, Accessed 2018.

[33] Wikipedia, *Puget sound faults.* https://en.wikipedia.org/wiki/Puget_Sound_faults, 2018.

[34] R. C. Witter, Y. Zhang, K. Wang, G. Priest, C. Goldfinger, L. Stimely, J. English, and P. Ferro, *Simulating tsunami inundation for a range of Cascadia megathrust earthquake scenarios at Bandon, Oregon USA*, Geosphere, 9 (2013), pp. 1783–1803.